Assessment of the sensitivity and uncertainty of equilibrium river state predictions:

A case study on the river Waal

P.S.J. (Philippine) van Tets

Delft University of Technology

TU Delft

HKV LIJN IN WATER

Assessment of the sensitivity and uncertainty of equilibrium river state predictions:

A case study on the river Waal

by

P.S.J. van Tets

to obtain the degree of Master of Science

at Delft University of Technology,

to be defended publicly on Monday September 6, 2021 at 12:00.

Student number:	4356446	
Thesis committee:	Dr. ir. A. Blom,	TU Delft, chair
	Dr. ir. A.J. Paarlberg,	HKV, daily supervisor
	Dr. ir. R.P. van Denderen,	HKV, daily supervisor
	Dr. R.M.J. Schielen,	TU Delft
	Dr. ir. R.J. Labeur,	TU Delft

An electronic version of this thesis is available at `http://repository.tudelft.nl/`.

Cover: the river Waal as seen from Beneden-Leeuwen.

TU Delft

Preface

This thesis is the last step in the finalization of my Master of Science in Hydraulic Engineering at Delft University of Technology with the specializations River Engineering and Coastal Engineering.

The topic of this study is the uncertainty and sensitivity of equilibrium state predictions, which is investigated for the river Waal. Predicting how rivers change towards their equilibrium state is important for long-term river management, however it is often overlooked. This thesis is hopefully a first step in making analytical relations a reliable method that can be used by river managers. I am grateful for the opportunity to combine my thesis with an internship at HKV.

I would like to thank my committee for their time, for reading and giving valuable feedback on my report and for their guidance. Andries en Pepijn, thank you for all the meetings we have had, for being closely involved, and for including me in HKV activities. Astrid has given valuable guidance, not only about this research but also on a personal level, for which I am very grateful. I would like to thank Ralph for asking questions that helped me to reflect on my work. Robert Jan, thank you for your help with restructuring my report.

Furthermore, I would like to thank HKV for including the students in (online) events; the student presentations are a good initiative, and I appreciate it that the students are included in the coffee breaks, the team meetings and the online drinks. And thank you Liselot for helping me to get started with the ELV code.

Finally, special thanks to my housemates and friends for their support and for distracting me on stressful moments. Thanks to Geerten for going with me to visit the Waal and for patiently listening to all my questions. And of course thanks to my family for giving feedback on my report and for their support and motivation.

Philippine van Tets
The Hague, August 2021

Summary

The natural development of the morphology of rivers in time is important due to the functions rivers fulfil, such as navigability and drinking water supply. Rivers adjust their morphology when there is a change in the river controls, which are mainly the water discharge, sediment discharge and downstream water level. The morphology adjustments continue until a river has reached its equilibrium state (i.e. equilibrium bed slope and equilibrium bed surface sand fraction), which is when all sediment that is supplied upstream of the river can be transported downstream.

Even though an assessment of how the river changes towards its equilibrium state is important for the performance of the functions of a river, it is often overlooked. This can for example lead to increased maintenance costs and dangerous situations. A quick method to calculate the equilibrium state of a river can help prevent these negative impacts. The analytical relations by Blom et al. (2017) are a promising method to predict how a river will change, since they give useful and rapid insight in the equilibrium river state.

However, the degree of uncertainty of the equilibrium river state as a result of the uncertainty in the input parameters is not yet known. It is recommended to examine this uncertainty before interpreting how a river will change. The aim of this research is therefore to investigate what the range of uncertainty of calculated equilibrium river states is, and to execute a sensitivity analysis to examine which input parameters contribute the most to this uncertainty. The river Waal is chosen as a case study for these analyses. The calculated equilibrium state of the river Waal, including the range of uncertainty, is compared to river state measurements to assess how well an equilibrium state can be identified.

A model is created based on the analytical relations, and is used to perform three different analyses; a deterministic analysis that results in a spatially varying equilibrium state without uncertainties, a sensitivity analysis that assesses the influence of each input parameter on the equilibrium state, and an uncertainty analysis that results in a bandwidth of possible equilibrium states.

The result of the sensitivity analysis is that the mean gravel content of the total sediment supply and the total sediment supply itself have the largest impact on the uncertainty of the equilibrium state. The result of the uncertainty analysis is that the equilibrium bed slope can be approximately $1.8 \cdot 10^{-5}$ smaller or larger than the mean bed slope, with an uncertainty bandwidth of approximately $3.7 \cdot 10^{-5}$, and that the equilibrium bed surface sand fraction can be approximately 10% to 20% smaller and 10% to 35% larger than the deterministic bed surface sand fraction, with an uncertainty bandwidth between 20% to 50%, depending on which sediment transport relation has been used.

From the comparison between the calculated equilibrium state, including uncertainties, and the measured river state, it follows that the current bed slope is steeper than the equilibrium bed slope, and that the current bed surface sand fraction is either larger than or within the uncertainty bandwidth of the equilibrium bed surface sand fraction. The found milder equilibrium bed slope is as predicted. However, the found equilibrium sand fraction does not match the prediction that the bed surface sand fraction is smaller in the equilibrium state.

From the comparison and the results of the uncertainty analysis follows that an equilibrium state cannot yet be identified, because 1) the uncertainty range of the calculated bed surface sand fractions is considered to be too large to predict the equilibrium state of the river Waal, and 2) the equilibrium bed surface sand fraction predictions do not match the expectation.

To improve the equilibrium state identification of the river Waal, it is recommended to 1) assess why there is a mismatch between the expected and calculated equilibrium bed surface sand fractions, 2) perform research to reduce the input uncertainty, and 3) validate the equilibrium state predictions.

Contents

1

Introduction

1.1. Context

Rivers in the Netherlands facilitate important functions such as navigation and drinking water supply. Navigation is important for the transportation of goods; in 2018 inland shipping contributed 17.9% to inland freight transport and 18.5% to freight transport across the Dutch border (CBS, 2018). Surface water contributes approximately 40% to the Dutch drinking water (Drinkwaterplatform, 2020). Next to these two functions, river flood events are a threat to approximately 60% of the Netherlands (Vergouwe, 2015). How well the river functions are fulfilled and how safe existing flood protections are, depends on the shape and planform of a river; the river morphology.

The morphological behaviour of a river can change over time and is determined by its controls. River controls mentioned by De Vriend (2015) are the time-varying upstream discharge, sediment input, downstream water level, geological constraints, vegetation in floodplains, engineering works and other human activities. When at least one of these controls change, the river will respond by adjusting the river flow and morphology.

The morphology of a river responds to changes in the controls by modifying the values of dependent variables, which can include the bed slope (and thus the bed level), the bed surface sediment composition, the shape and area of the cross-section, the planform pattern and the bed roughness (De Vriend, 2015). Engineered rivers, such as the Dutch Rhine branches, have a constrained planform and a fixed channel width, which means that they are unable to change their cross-section and planform pattern. These rivers can therefore only change the bed slope, the bed surface sediment composition and the bed roughness as a response to changes in the river controls.

The response of a river in time due to a change in the controls can be divided into short-term, transient and long-term effects. During the short-term response, only the river flow responds to the changes, as the river morphology has no time to adjust in this time scale. The order of magnitude of this time scale is days. The long-term response is when the river is adjusted to its equilibrium state, which is a stable channel form where the time-averaged amount of sediment that enters the river upstream is equal to the time-averaged amount of sediment that is transported downstream (e.g., Buffington, 2012). It might take centuries to reach this equilibrium state (e.g., Jansen et al., 1994). The transient response is the phase between the short-term and the long-term responses, where the river adjusts to changes in the controls in order to approach its equilibrium state (e.g., Blom et al., 2017).

Because the river functions and flood safety depend on the river morphology, it is important to investigate what the long-term river response is due to changes in the controls. However, the impact of the long-term and large-scale river response is often ignored (De Vriend, 2015). This ignorance is problematic, because a change in the controls can result in higher maintenance costs or even dangerous situations. An example of

a change in a river control that has led to a new equilibrium state with unforeseen problems is the narrowing of the Dutch Rhine branches (De Vriend, 2015). The channel narrowing that took place at the end of the 19th and start of the 20th century was designed to improve the navigability by increasing the water depth. The depth increased indeed, however the channel narrowing also contributed to a gradual reduction of the bed slope of the river. This has subsequently led to bed level lowering at the upstream side of the river, which has caused navigability problems near the Dutch-German border due to non-erodible layers. According to De Vriend (2015), the slope reduction could have been anticipated by using analytical equilibrium equations.

Analytical equilibrium relations could be a solution to the problem that the long-term river response is often ignored, because they can be used to rapidly calculate the equilibrium state of a river that is not in its equilibrium state yet. By comparing the values of the dependent variables in the predicted equilibrium state to measured values of the current river state, it can be examined how the river will change, and whether that would result in possible negative consequences.

The analytical relations by Blom et al. (2017) are possibly a suitable solution, because they give rapid and useful insight on the equilibrium river state and on the possible consequences of changes in the controls in the long-term (Blom et al., 2017). However, it is not yet known what the degree of uncertainty of the predicted equilibrium state is, and which input parameters contribute the most to this uncertainty. Due to the lack of information on the degree of uncertainty of the equilibrium state calculations, it is not known how well an equilibrium state calculated with the analytical relations by Blom et al. (2017) can be used to predict how a river will change compared to the measured river state.

If the analytical relations are applied without knowing the uncertainty range of the equilibrium state, there is a risk that the predicted long-term impact of a change in controls is different from the actual long-term impact. Possible measures that are implemented to reduce the predicted long-term impact could in that case work less well or even lead to negative consequences. This problem should be prevented by researching the uncertainty related to equilibrium state predictions from the analytical relations by Blom et al. (2017).

1.2. Problem statement

The consequences of the long-term river response to changes in river controls are often ignored (De Vriend, 2015), which can lead to problems for the important river functions. A possible solution for this problem is to calculate the equilibrium state of a river using the analytical relations by Blom et al. (2017), and to compare it to the current river state to investigate the possible consequences of the changes in river controls. Once the consequences are identified, mitigation measures can be designed and implemented to prevent problems in the future.

However, the degree of uncertainty of the equilibrium river state calculated with the analytical relations by Blom et al. (2017) is not known yet, nor which input parameters contribute the most to this uncertainty. It is therefore also not known if the calculated equilibrium state can be used to assess how the river will change to reach its equilibrium state, or whether the river is already in its equilibrium state. This should be investigated before a study can be conducted to assess how well the analytical relations can predict the impact of changes in river controls on the long-term.

1.3. Research objective

The aim of this study is to give insight in the range of uncertainty and the sensitivity of equilibrium state calculations with the analytical relations by Blom et al. (2017), due to uncertainties in the input parameters. The range of uncertainty is used in a comparison of the equilibrium state to measurements of the river state, in order to assess how well the calculations can indicate if a river has reached its equilibrium state. A river that has probably not yet reached its equilibrium state is chosen as a case study, which implies that we expect that the equilibrium state calculations including uncertainties do not match with the river state measurements.

The objective is translated into the main research question and four sub-questions. The main research question is:

How well can we assess whether an equilibrium state prevails along a river reach?

The following sub-questions help to answer the main research question:

1. What is the range of applicability of the analytical relations?
2. How sensitive is the predicted equilibrium state to uncertainty in the input parameters?
3. What is the range of uncertainty of the predicted equilibrium state?
4. How does the predicted equilibrium state compare to measured data?

1.4. Methodology

This section first introduces the case study and explains how the equilibrium and measured river states are defined, and subsequently gives the approach to answer the research questions.

For this research a case study is needed on which the analytical relations can be applied. The river Waal, which is a Dutch branch of the Rhine River, is chosen as the case study. It is a suitable river for this research due to extensive measurement campaigns and model simulations. From these available data, only the years up to the year 2014 are included in the equilibrium state calculations, due to large scale interventions of the project Room for the River after 2014. To prevent that short-term river responses have influence on the measured state of the river Waal, data from after the year 2014 are excluded. Even though the data of these most recent years are excluded, we refer to the measured state as the current state of the river Waal.

The equilibrium state and the measured state of the river Waal are defined by dependent variables as explained in Section 1.1. The dependent variables that are included in the analytical relations by Blom et al. (2017) are the bed slope, width, and bed surface sediment composition. Because the river Waal is an engineered river, the width is constant and thus not a dependent variable in this case. The equilibrium state and measured state of the river Waal are therefore defined by the bed slope and bed surface sediment composition.

This thesis starts in Chapter 2 with an explanation of background information, which encompasses a description of equilibrium classification and flow segments, and an overview of possible methods to predict an equilibrium state.

The approach of this thesis to answer the research questions is described in Figure 1.1. The river Waal is introduced in Chapter 3, where the exact region is determined that is used as case study. For this region the measured river state is examined. The applicability of the analytical relations on the case study is analysed in Chapter 4, which gives answer to the first sub-question. Next to that, a model is created that calculates equilibrium states for the river Waal, with input that is based on the case study.

There are three separate analyses performed to predict the equilibrium state of the river Waal, of which the results are given in Chapter 5. The first one is a deterministic analysis, which results in a spatially varying deterministic equilibrium state where no uncertainties are included. The second analysis examines the sensitivity of the calculated equilibrium state based on uncertainties in the input parameters. The resulting sensitivity of the equilibrium state answers the second sub-question. The third analysis is an uncertainty analysis, where an equilibrium state bandwidth is calculated by combining the uncertainty ranges of certain parameters. The results of this third analysis answer the third sub-question. Due to a longer computation time, the uncertainty analysis is only used to calculate the bandwidth for one location at the river Waal, which means that the result of this analysis is not spatially varying. To answer the fourth sub-question, the measured state of the river Waal is compared to the deterministic equilibrium state, combined with the uncertainties from the uncertainty analysis.

After the presentation of the results in Chapter 5, they are discussed in Chapter 6. Answers to the research questions and recommendations are given in Chapter 7.

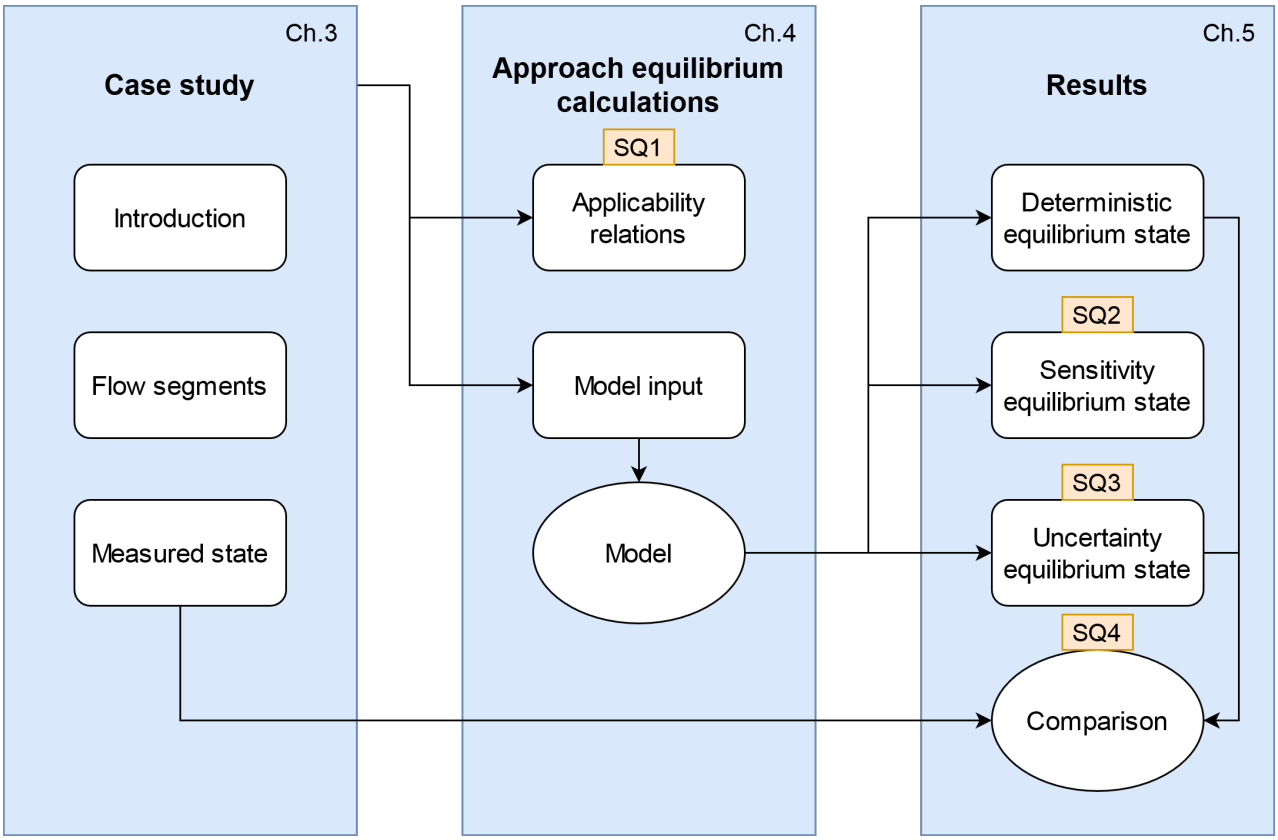

Figure 1.1: Schematic overview of the methodology used in this study. Chapters are indicated by the abbreviation Ch., and sub-questions by the abbreviation SQ. The main question can be answered at the end of this research.

2

Literature study

This chapter provides relevant background information on flow segments and equilibrium classifications in Section 2.1 and it discusses the literature on analytical equilibrium relations in Section 2.2.

2.1. Equilibrium classification and flow segments

This section gives background information on the different types of equilibria that can be distinguished and on the flow segments that a river consists of. The equilibrium classification is relevant to place this study in the context of previous research on equilibrium predictions. Information on the flow segments is required to understand the differences between some analytical relations.

There are four different types of equilibrium states that can occur, which are illustrated in Figure 2.1 (Arkesteijn et al., 2019); a static equilibrium, a dynamic equilibrium, a static quasi-equilibrium and a dynamic quasi-equilibrium. In a static equilibrium state, the controls of a river remain constant in time, resulting in a constant bed surface sediment composition, river width and bed slope. If the river controls change in time, but at a rate that is slow relative to the timescale of the river response, the river is in a static quasi-equilibrium state. In this case the river geometry can keep pace with the change in controls. When the controls fluctuate over short timescales around a constant value, the river is in a dynamic equilibrium state. This state is characterized by fluctuations in bed slope, width (in a non-engineered river) and bed surface sediment composition around a mean value. If the controls fluctuate over short timescales around slowly changing values with respect to the timescale of the river response, the river is in a dynamic quasi-equilibrium state. In this state the river geometry fluctuates around slowly changing mean values (e.g., Howard, 1982; Blom et al., 2017; Arkesteijn et al., 2019).

In this study, the equilibrium state of the river Waal is calculated for river control values that correspond to a specific moment in time. Because changes of the river controls in time are not within the scope of this study, it is not necessary to know whether a static or quasi-static equilibrium state will prevail along the river Waal. This could be important for example if the development of the river Waal in time is part of the research objective, or if one wants to predict the equilibrium state of a river in a specific moment in the future for yet unknown river controls. It is generally known that the controls of the river Waal show fluctuations, which indicates that the river Waal is heading towards a dynamic equilibrium state with river geometry that fluctuates around a mean value. In this study we are interested in the mean river geometry values of an equilibrium state and its corresponding uncertainty. This uncertainty originates partly from variations in the river controls, and is thus related to the dynamic fluctuations. For clarity, the dynamic and possibly quasi-equilibrium state of the river Waal is in the remainder of this report referred to as the equilibrium state of the river Waal.

The equilibrium state of the river Waal is not only influenced by its controls, but also by the Pannerdense

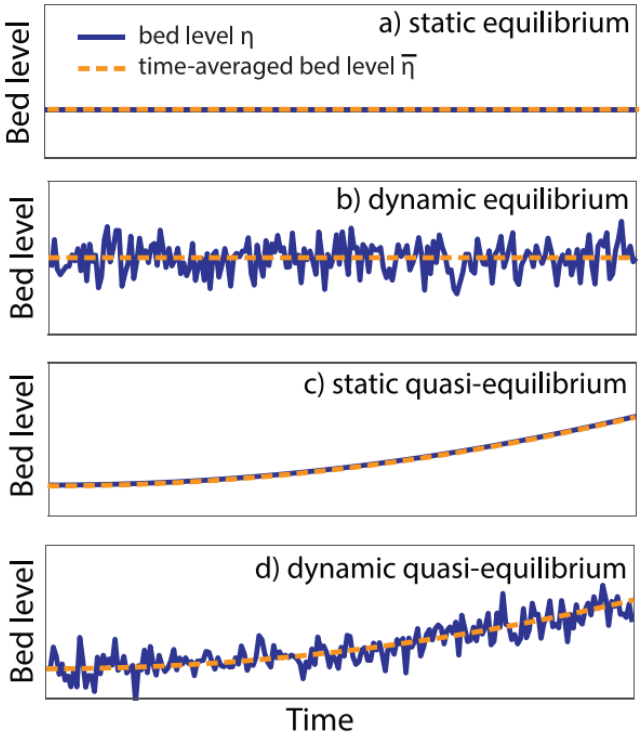

Figure 2.1: Schematics for different types of equilibria. From Arkesteijn et al. (2019).

Kop bifurcation at the upstream end of the river Waal. The distribution of sediment over the two downstream branches of a bifurcation determines if both branches remain open, or if one branch silts up towards the equilibrium state. For an engineered river with unisize sediment there are three possible equilibrium solutions, whereas three to five equilibrium states exist for mixed-size sediment (Schielen and Blom, 2018). For the development towards one of these equilibrium states it is however implied that there are no human interferences. We assume that the Dutch water authorities will prevent the silting up of either of the branches downstream of the Pannerdense Kop bifurcation, presumably by maintaining the water and sediment distribution between the branches. This means that we expect that the distribution of water and sediment at the Pannerdensche Kop bifurcation will remain approximately stable in the future, and we therefore assume that there is only one possible equilibrium state for the river Waal.

A river can be divided in three types of zones: a backwater segment, a normal flow segment, and a hydrograph boundary layer (HBL) (e.g., Blom et al., 2017; Arkesteijn et al., 2019), as illustrated in Figure 2.2. Backwater segments are influenced by the downstream water surface base level; a backwater curve forms when this base level deviates from the normal flow depth (e.g., Blom et al., 2017). Backwater segments not only form where the river enters a lake or sea, they also occur upstream of confluences, bifurcations and at locations where the river geometry or friction vary spatially (e.g., Arkesteijn et al., 2019). The HBL, sometimes also called the upstream boundary segment, is a reach where the instantaneous sediment supply rate is not equal to the instantaneous sediment transport capacity, even though the time-averaged sediment supply rate and transport capacity do match. This results in continuous adaptations of the bed elevation and bed surface sediment composition, with bed degradation and bed surface coarsening during higher flows and bed aggradation and bed surface fining during lower flows (e.g., Arkesteijn et al., 2019; An et al., 2017). A normal flow segment is the area where both the upstream and backwater boundary effects are negligible and where the flow is uniform at each flow rate, which means that the flow velocity is constant in space, even though the flow rate varies in time (e.g., Arkesteijn et al., 2019). This segment can be approximated as normal or uniform, which implies that the friction slope is approximately equal to the bed slope and that there are no bed elevation changes (e.g., Blom et al., 2017).

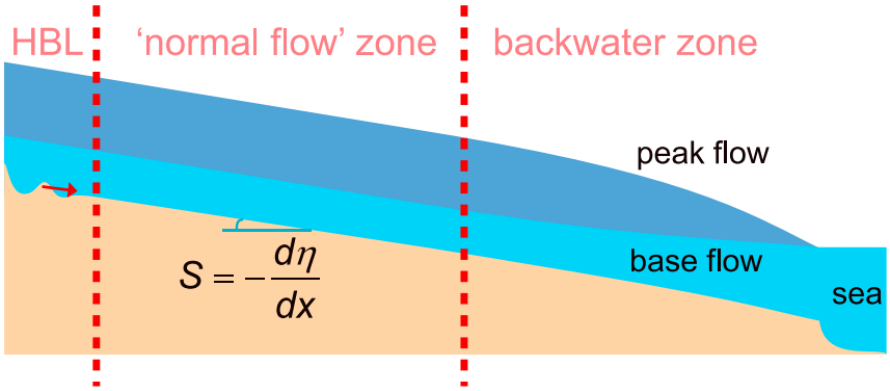

Figure 2.2: Schematic of the three flow segments: the hydrograph boundary layer (HBL), the normal flow zone, and the backwater zone. From Blom et al. (2017).

2.2. Analytical equilibrium relations

Predicting the equilibrium state of a river is possible with either numerical models (e.g., Viparelli et al., 2011; Bolla Pittaluga et al., 2014; Lanzoni et al., 2015; Nones et al., 2019) or analytical relations (e.g., Howard, 1980; Jansen et al., 1994; Blom et al., 2017; Arkesteijn et al., 2019).

Numerical models can calculate the equilibrium state by running a morphological river simulation for a sufficiently long time without changing the river controls. When the morphology does not change anymore in the model, the river has reached its equilibrium state. Viparelli et al. (2011) for example have used a numerical model to calculate the equilibrium state of a river reach of approximately 10 km. To reach the equilibrium state of that river reach, simulations of 1800 to 15,000 years were necessary. Church and Ferguson (2015) find similar time scales, stating that 1000 to 10,000 years are required for a 100 km long river to adjust to changes in the controls. A disadvantage of numerical models is that simulations of these durations also require a long time to run; a simulation can take even more than a month of computation time. Because several simulations are needed in this research to analyse the sensitivity and uncertainty related to the equilibrium state of the river Waal, numerical models are in this case not suitable.

Analytical equilibrium relations on the other hand require almost no computational time, because they usually calculate the equilibrium state of a river without the transient response. Analytical relations that are possibly suitable for predictions of the equilibrium state of river reaches are the relations by Blom et al. (2017) and Arkesteijn et al. (2019). The relations by Blom et al. (2017) can predict the equilibrium bed slope and bed surface sediment composition under variable flow, and are an extension of the analyses by Jansen et al. (1994), De Vries (1993), Howard (1980) and Doyle and Shields (2008) to multiple sediment fractions. Furthermore, these relations are an extension to the Blom et al. (2016) relations for equilibrium geometry to variable flow rate. However, a limitation of these relations is that they are only suitable for normal flow segments. The analytical relations by Arkesteijn et al. (2019) are able to assess equilibrium river geometry in both normal flow and backwater segments by using a space-marching method, which solves the equilibrium channel geometry from downstream to upstream. The relations as described in their study are only applicable to unisize sediment, however a version with mixed-size sediment is available. A limitation of these relations is that it is not known how the space-marching method might accumulate uncertainties in upstream direction, making it more difficult to assess how uncertain the predicted equilibrium state is. Furthermore, it is assumed that it is more difficult to get a grip on how to use these relations with respect to the relations by Blom et al. (2017). Due to these two difficulties, we have chosen to use the analytical relations by Blom et al. (2017) in this study. However, we expect that the relations by Arkesteijn et al. (2019) could also be used to answer the research questions.

3

Case study: river Waal

The case study, the river Waal, is introduced in this chapter. The general characteristics of the river Waal are identified in Section 3.1. Section 3.2 examines whether an equilibrium state prevails along the river Waal based on measurements. Because the analytical relations by Blom et al. (2017) are only applicable on normal flow segments of a river, the flow segments are identified in 3.3. The measured bed slope of the river Waal is derived from bed elevation measurements in Section 3.4, and the measured bed surface sediment composition is given in Section 3.5. These two sections combined form the measured state of the river Waal.

3.1. Characteristics river Waal

The river Waal is a branch of the river Rhine situated in the Netherlands. The branch starts at the Pannerdense Kop bifurcation, where the river Bovenrijn splits into the river Waal and the river Pannerdensch Kanaal. From this bifurcation, the river Waal flows to Woudrichem, where its name changes to the Boven-Merwede. At Werkendam the river Boven-Merwede bifurcates into the river Beneden-Merwede and the river Nieuwe Merwede. In this research the river Boven-Merwede is included in the study area and is also called the river Waal. The total length of the river Waal including the river Boven-Merwede is approximately 90 km. Expressed in riverkilometers, the river Waal extends from rkm 867 at the upstream end to rkm 960 at the downstream end, which is illustrated in Figure 3.1.

The average main channel width of the river Waal is approximately 300 m, and the average navigation channel width is roughly 150 m. The mean discharge at Lobith, which is located just upstream from the Pannerdense Kop bifurcation, is approximately 2200 m^3/s (for the years 1901 until 2013, data courtesy: Rijkswaterstaat, data obtained from the Global Runoff Data Centre). The percentage of discharge that flows from the river Bovenrijn into the river Waal depends on the amount of discharge upstream, but it is on average 2/3 of the total discharge (Figure 3.2; e.g., Arkesteijn et al., 2019).

There are three permanent bed interventions present along the river Waal, situated in the outer corner of a bend. The first intervention consists of submerged groynes near Erlecom, between rkm 873 and rkm 876. The second and third interventions are non-erodible layers, one is situated near Nijmegen between rkm 883 and rkm 885, and the other is at St Andries between rkm 925 and rkm 928 (e.g., Van Reen, 2002). All three interventions are referred to as non-erodible layers in the remainder of this report. The non-erodible layers help to maintain the river bends, however they cause extra erosion downstream of the layers. Due to the local disturbances they can create, it is important to take these layers into account when analysing the river state.

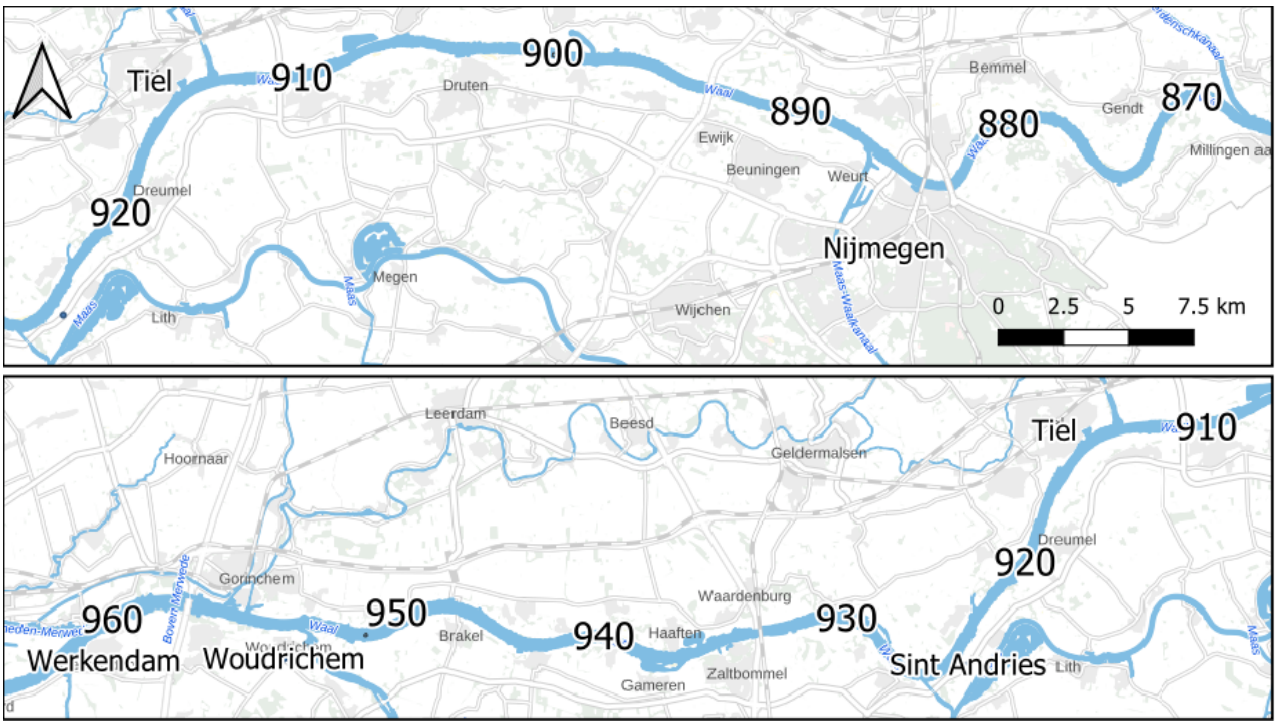

Figure 3.1: The Waal branch of the river Rhine, from rkm 867 at Pannerdense Kop to rkm 960 near Werkendam. The left side of the top image continues at the right side of the bottom image.

Figure 3.2: The Pannerdense Kop bifurcation. Approximately 2/3 of the discharge at the river Bovenrijn flows into the river Waal, indicated by the red arrow. The remainder of the water flows into the river Pannerdensch Kanaal, indicated by the blue arrow.

3.2. Identification current state

In this section, we analyse whether the river Waal has already reached its equilibrium state. First, we discuss how the state of a river can be identified based on measurements. Subsequently the state of the river Waal is examined, and finally a conclusion is made on whether the river Waal has reached its equilibrium state.

Three methods are used in this research to identify the state of the river Waal. The first two methods are based on the definition that river geometry and morphology are constant or change slowly in an equilibrium

state (Figure 2.1; e.g., Arkesteijn et al., 2019). Method one analyses whether there are large-scale natural changes in time to the river geometry, which would be an indication that the river Waal has not yet reached its equilibrium state. The second method investigates if there are large-scale natural changes in the river morphology, by analysing the bed surface sediment composition of the river Waal in time. The third method is based on the definition that all sediment that enters a river upstream must also be transported downstream if the river is an equilibrium state (e.g., Buffington, 2012). This means that a mismatch between time-averaged sediment supply and sediment transport indicates that the river has not yet reached its equilibrium state.

To analyse the river geometry of the river Waal in time for method one, we use measurements of the bed elevations and bed slope of the Lower Rhine River between the years 1898 and 2018 as presented by Ylla Arbós et al. (2020), see Figure 3.3. Ylla Arbós et al. (2020) find a bed level and bed slope reduction at the river Waal that is still ongoing. This leads to the assumption that the river geometry is changing considerably and thus that the river Waal is not in an equilibrium state yet.

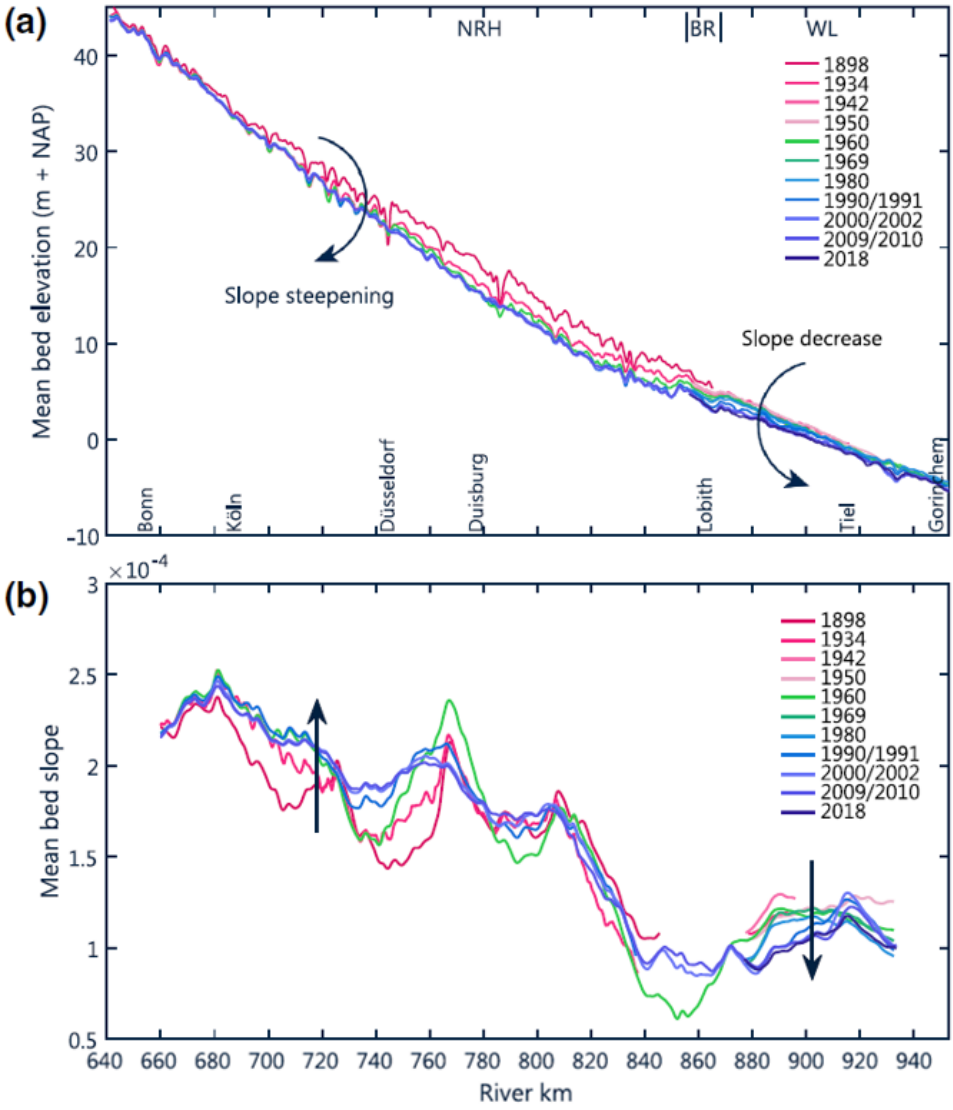

Figure 3.3: Bed elevation and bed slope in the Lower Rhine River over the past century: (a) bed elevation, moving average with window size 2 km; (b) bed slope, moving average with window size 40 km. The Niederrhein, Bovenrijn, and Waal reaches are indicated with labels NRH, BR, and WL, respectively. From Ylla Arbós et al. (2020).

Bed surface sediment composition data would be most suitable to perform method two, however there are not sufficient measurements in time to analyse if large-scale changes have taken place. Therefore, measurements of the median bed surface grain size D_{50} over the past few decades are used, see Figure 3.4. A higher median

bed surface grain size is an indication that the coarser bed surface sediment fractions are larger than the finer bed surface sediment fractions.

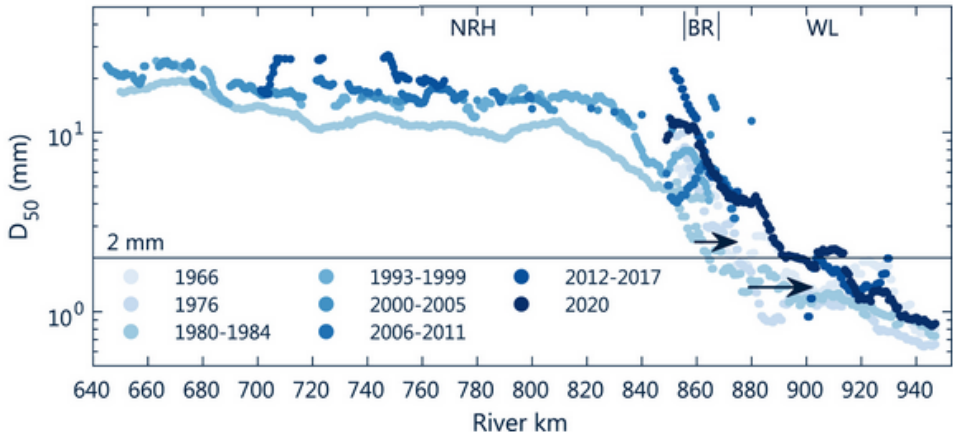

Figure 3.4: Median bed surface grain size D_{50} in the Lower Rhine River over the past century. The Niederrhein, Bovenrijn, and Waal reaches are indicated with labels NRH, BR, and WL, respectively. From Ylla Arbós et al. (2020).

It can be observed in Figure 3.4 that the median grain size has become coarser over the years along the river Waal. Furthermore, a movement of coarser sediment grain sizes in downstream direction is visible, indicated with the two arrows. This is the movement of the gravel-sand transition, which has caused a transformation of the river Waal from a sand-bed river to a gravel-bed river up to Tiel over the past decades (Ylla Arbós et al., 2020). Even though a flattening of the gravel-sand transition is observed (Ylla Arbós et al., 2020), we assume that the median grain size at the bed of the river Waal will increase in the future. The coarsening of the river bed surface is an indication that the river Waal has not yet reached its equilibrium state, and that an increase in the coarser bed surface sediment fractions with respect to the finer bed surface sediment fractions is expected.

For the analysis of the time-averaged sediment supply and transport in method three, we look at the sediment balance for gravel and sand in the Rhine delta for the years between 1991 and 2010 (Frings et al., 2015). The sediment balance for the river Waal can be defined as:

$$I_{up} - O_{fl} - O_{dr} - O_{do} = \Delta S \tag{3.1}$$

where I_{up} (Mt/a) is the sediment input from upstream, O_{fl} (Mt/a) is the sediment output due to sedimentation on floodplains, O_{dr} (Mt/a) is the sediment output due to dredging, O_{do} (Mt/a) is the sediment mass leaving the river Waal at the downstream end and ΔS (Mt/a) is the sediment mass stored in the river. With the values for the sediment balance terms indicated in Figure 3.5, the sediment mass stored in the river Waal is ΔS = -0.17 Mt/a, which implies that more sediment mass leaves than enters the river. This should result in erosion of the river bed, which corresponds to the bed level lowering of the river Waal found by Ylla Arbós et al. (2020), leading to the assumptions that the river Waal has not reached its equilibrium state yet. However, it should also be noted that the uncertainty related to the sediment balance terms is approximately 50% (Frings et al., 2015). This means that it is also a possibility that the sediment transport upstream and downstream of the river Waal are approximately equal. Therefore, even though the sediment transport data appear to indicate that the river Waal is not in its equilibrium state, no final conclusion can be made about the equilibrium state based on sediment transport values.

Based on our analysis of the river geometry, the river morphology and the sediment transport data, it is very likely that the river Waal is still adapting towards its equilibrium state. We therefore assume for the remainder of this study that the river Waal has not reached its equilibrium state yet.

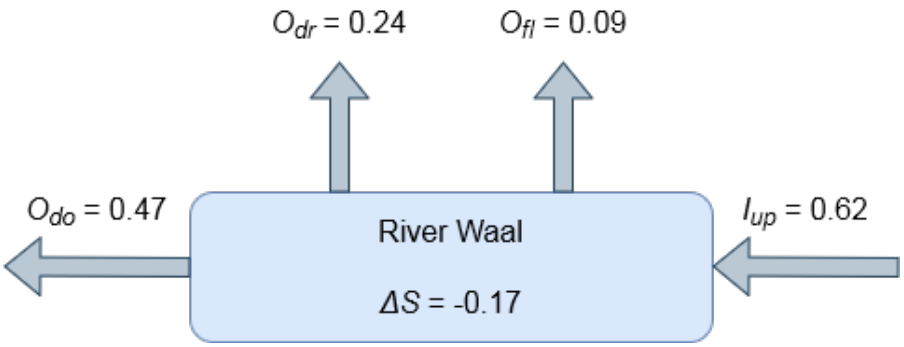

Figure 3.5: Sediment balance for the river Waal expressed in Mt/a; the sediment mass entering the river (I) minus the sediment mass leaving the river (O) equals the sediment mass stored in the river (ΔS). Adapted from Frings et al. (2015).

3.3. Flow segments

As mentioned in Section 2.2, the analytical relations by Blom et al. (2017) only hold for normal flow segments. It is unknown how well these relations can be used to predict an equilibrium state in the HBL and backwater segments, and it is thus recommended to only apply them to a normal flow segment of the river Waal. In this section, the flow segments of the river Waal are distinguished. This section is subdivided into a method to identify the normal flow segment, the application of the method to the river Waal, the results of the normal flow identification and finally a criterion that can be used to identify normal flow segments.

3.3.1. Flow segment identification approach

There are no equations or criteria to easily distinguish the flow segments of a river. To identify these segments, we create a method based on the differences in the definitions of the three types of river segments. As mentioned in Section 2.1, a backwater segment is defined by a backwater curve, which is a curvature of the water surface h (m). An HBL is defined by changing bed elevations z_b (m) and bed surface sediment composition. A normal flow segment is defined by uniform flow, where the bed slope i_b (-) is approximately equal to the friction slope i_f (-), which is the streamwise derivative of the energy head H (m). Because the flow velocity u (m/s) is constant in space in uniform flow, these slopes are also identical to the water surface slope i_w (-). Identical bed and water surface slopes imply that the water depth d (m) is constant in longitudinal direction. The slopes and elevations mentioned above are illustrated in Figure 3.6.

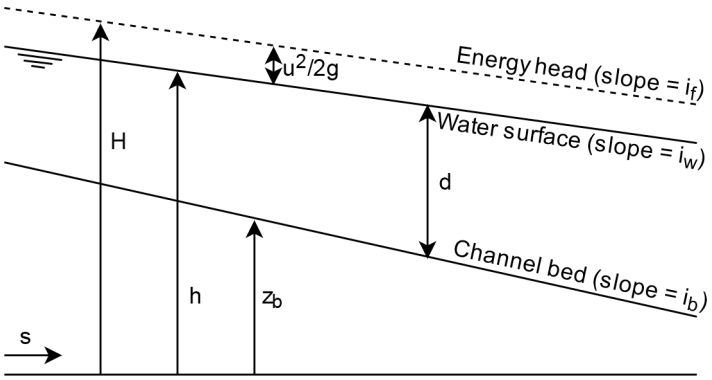

Figure 3.6: Illustration of various slopes and elevations in a river. The slope of the energy head is called the friction slope, i_f. The streamwise direction s is towards the right in this case.

A method to distinguish between the three types of segments, based on their definitions, is to analyse measurements of the water surface and bed elevations of a river; a location where a backwater curve is present is a backwater segment and a location where the bed slope and water surface slope are approximately equal is a normal flow segment. An HBL is more difficult to determine, because the bed elevation varies around an average bed elevation with an average bed slope that is likely equal to the water surface slope. This can give

the impression that a normal flow segment is present. It is also not known how large these bed elevations are with respect to other natural bed variations such as ripples, and whether they are visible in bed elevation measurements. Due to these difficulties, we distinguish an HBL as a river reach that is not a normal flow segment due to different bed and water surface slopes, and that is not a backwater segment due to a straight water surface slope. If an HBL is falsely identified as a normal flow segment due to an approximately equal bed and water surface slope, the consequence is limited for this study. This is because the analytical relations by Blom et al. (2017) are limited to normal flow segments due to the use of the normal flow equation, which is only applicable for river reaches where the bed and water surface slope are equal.

3.3.2. Application of approach to river Waal

For the identification of the flow segments of the river Waal, we use bed level and water surface measurements. Biweekly multi-beam measurements of the bed elevation of the river Waal from the years between 2005 and 2014 are used to obtain bed level values that are representative for the state of the river Waal before the Room for the River interventions. The measurements are first spatially averaged over the cross-section of the 150 m wide navigation channel of the Waal and every 5 m in the longitudinal direction. After that, the biweekly measurements are averaged in time. This results in temporally averaged bed levels with a longitudinal resolution of 5 m.

Water surface level measurements for the river Waal are obtained from a dataset called *betrekkingslijnen* for the years 2012 up to 2014 (data courtesy: Rijkswaterstaat). These water levels have been measured at several measurement stations along the river Waal during various water discharges Q (m^3/s), and are interpolated in space and between discharges. Because the presence and extent of backwater curves depend on the discharge (Battjes and Labeur, 2017), we want a range of discharges that represent frequently occurring flow situations. For this reason, the 5%, 50% and 95% quantiles of the past 100 years of discharge measurements at Lobith are used. This corresponds approximately to discharges of 1000 m^3/s, 2000 m^3/s and 4500 m^3/s respectively. The water surface levels corresponding to these discharges and the temporally averaged bed levels are shown in Figure 3.7, where the levels z (m) are given with respect to the *Normaal Amsterdams Peil* (NAP).

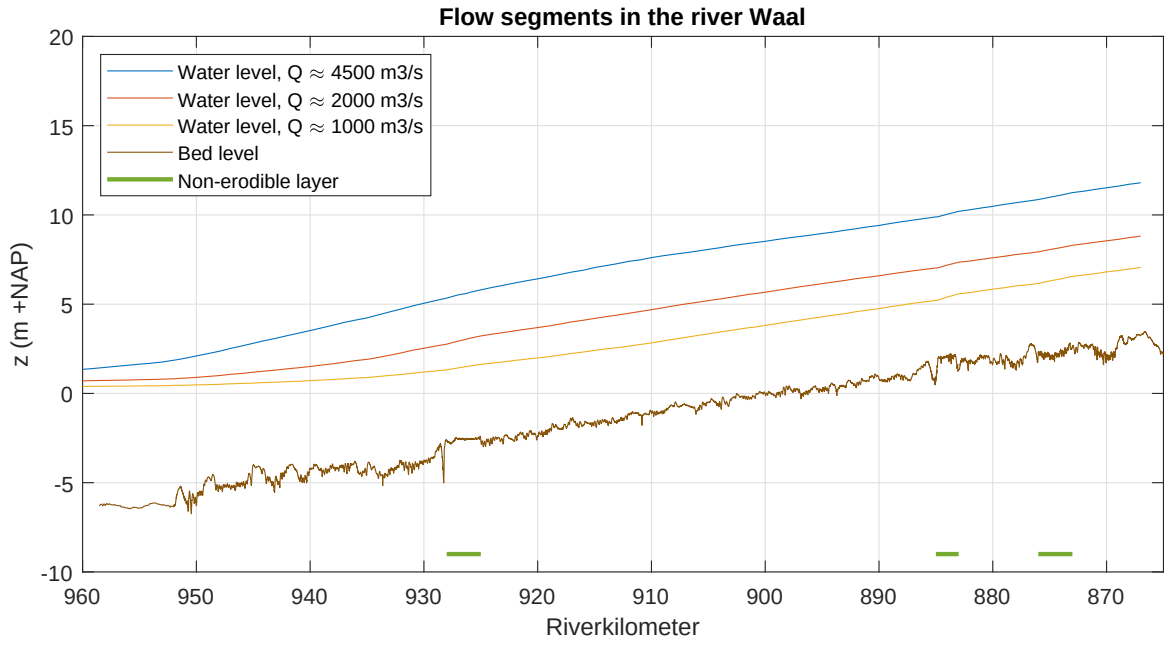

Figure 3.7: Measured bed levels and water surface levels of the river Waal. The locations of the non-erodible layers are indicated with green lines near the x-axis.

The non-erodible layers are indicted in Figure 3.7 as green horizontal lines. The non-erodible layer at St Andries, between rkm 925 and rkm 928, is clearly visible in the bed level measurements due to the constant

bed levels within that region and due to a sharp decline in the bed levels directly downstream, hinting at strong erosion behind the non-erodible layer. The same sharp decline in bed levels is visible downstream of the non-erodible layer near Nijmegen, between rkm 883 and rkm 885. The bed levels at that location appear to be constant as well, however less distinctive than at the layer near St Andries. The submerged groynes near Erlecom, between rkm 873 and rkm 876, do not seem to have a strong effect on the bed elevations.

3.3.3. Results flow segment identification

When analysing the bed elevations and water surface levels in Figure 3.7, the backwater curves at the downstream area of the river Waal are noticeable for all three discharges. These water surface curvatures are present from the downstream end at rkm 960 until somewhere between rkm 930 and rkm 910. We choose to identify rkm 920 as the start of the backwater curves, and thus to identify the river reach between rkm 920 and rkm 960 as a backwater segment.

Along the remainder of the river Waal, between rkm 867 and rkm 920, the water surface slope appears to be approximately constant. However, the bed slope between rkm 867 and rkm 885 seems to be slightly milder than the bed level slope between rkm 885 and rkm 920. Because the water surface slope and bed slope appear to be approximately equal between rkm 885 and rkm 920, this river reach is identified as a normal flow segment. The upstream river reach, between rkm 867 and rkm 885 is identified as an HBL, since there is no backwater curve present and there is a small difference in bed and water surface slopes. The flow segments of the river Waal are indicated in Figure 3.8. All three non-erodible layers are outside the normal flow segment, and are therefore not considered in the remainder of this research.

The HBL identification is however a rough estimation, because we have not determined whether the bed elevation variations that are characteristic for an HBL are present in that area, and because the water surface and bed slopes are still quite similar. It is thus also possible that this river reach is partly or fully a normal flow segment. However, no additional research is done to better indicate this river reach, because it is more important for this research to include a river reach as study area that conforms best to the analytical relations by Blom et al. (2017), than to include all areas that are possibly a normal flow segment. This means that the area between rkm 885 and rkm 920 is the normal flow segment that is used as study area in the remainder of this research.

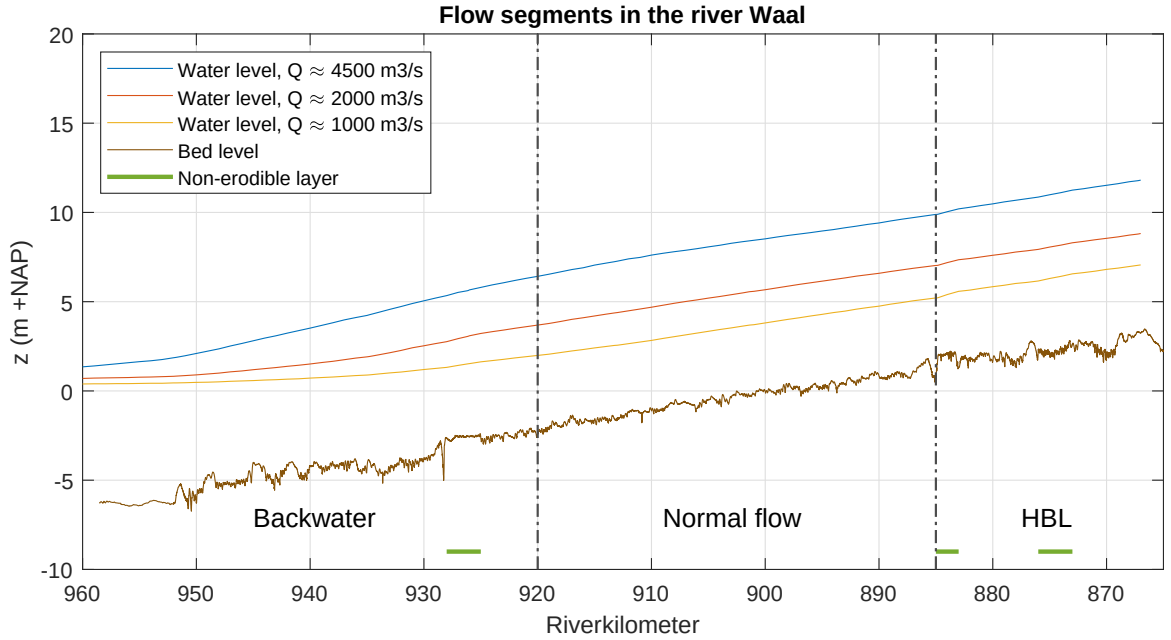

Figure 3.8: The identified flow segments of the river Waal. The segments are separated from each other by the dash-dotted lines.

3.3.4. Normal flow segment identification criterion

The identification of the different flow segments of the river Waal as described above is based on visualisations and therefore not very well fit for reproduction. To improve this and to create the possibility for a faster identification of the possible normal flow segments in other rivers, a normal flow segment identification criterion is created. The criterion is, similarly to the visual identification, based on the definition that the bed slope is approximately equal to the friction slope in a normal flow segment. It is assumed that the smaller the difference between the bed and friction slope is, the more likely it is that the region is a normal flow segment. The normal flow criterion is based on this idea; a region with a slope difference that is smaller than the criterion is a normal flow segment, and a region with a higher slope difference is either a backwater segment or an HBL.

The aim of the criterion is that it can be applied to other rivers as well, which implies that the slope difference must be a relative difference. To obtain this relative difference, the absolute difference between the slopes must be divided by a certain function of the bed and friction slopes. The choice has been made to divide the absolute difference by the maximum absolute value of the two numbers. The relative difference d_r (%) is thus defined as:

$$d_r = \frac{|i_b - i_f|}{\max(|i_b|, |i_f|)} \cdot 100\% \tag{3.2}$$

For the criterion analysis a higher precision is required than for the visual identification of the segments, and it can therefore not be assumed that the flow velocity is constant in space. This means that, opposed to the visual identification, the water surface slope cannot be used instead of the friction slope, and thus information on the friction slope is needed. There are no direct measurements of the energy head or the friction slope available, and it is therefore decided to use a WAQUA simulation that has information on the energy head with corresponding bed levels.

WAQUA is a model that can be used for 2D hydrodynamic modelling in rivers. A 2D simulation of the river Waal of the year 2014 is used for the criterion analysis. The energy head varies with the discharge, which means that at least two discharges are needed to represent the variation in energy head due to different discharges. The available discharges in the WAQUA simulation are 2000, 4000, 6000, 8000 and 10,000 m^3/s at Lobith, which means that unfortunately not the same discharges can be used as for the visualisation of the river segments. To resemble these discharges the most, the WAQUA simulations with discharges of 2000, 4000 and 6000 m^3/s are used in this study.

The WAQUA energy heads and bed levels are given in 2D, however only 1D data is needed, which means that the data from the simulation has to be converted. 1D energy head levels are obtained by selecting the energy head values at the river axis, assuming that the water surface levels and velocity, which together form the energy head, are approximately constant over the channel width. It can however not be assumed that the bed level data from WAQUA is approximately constant in the channel cross-section, because the bed levels have large variations in both cross-sectional and longitudinal direction. The bed level differences over the width have to be averaged out before the 2D bed levels are converted to 1D values. The cross-sectional averaging and the conversion to 1D results in an average bed level value every 100 m along the river Waal. The 1D energy head and bed level values are shown in Figure 3.9.

To calculate the bed slope from the obtained 1D bed levels, three processing steps are performed. The first step is to apply a moving average of 20 km, which is necessary to smooth the wiggles that are present in the bed levels, while maintaining large-scale spatial differences. A downside of using a moving average is that in this case the most upstream and downstream 10 km are less representative, since there are no data values available further up- and downstream respectively to use in the moving average. This has however no consequences to this approach, since the most upstream and downstream 10 km are outside the normal flow segment. The second step is to calculate the bed level slope per kilometer. This is done by applying a linear fit to all data points within a kilometer and to repeat this for all kilometers along the river Waal. The last step is to average the slopes to decrease the influence of possible outliers, which is done by applying a moving average of 10 km. The combination of both moving averages results in a less representative river reach of 15

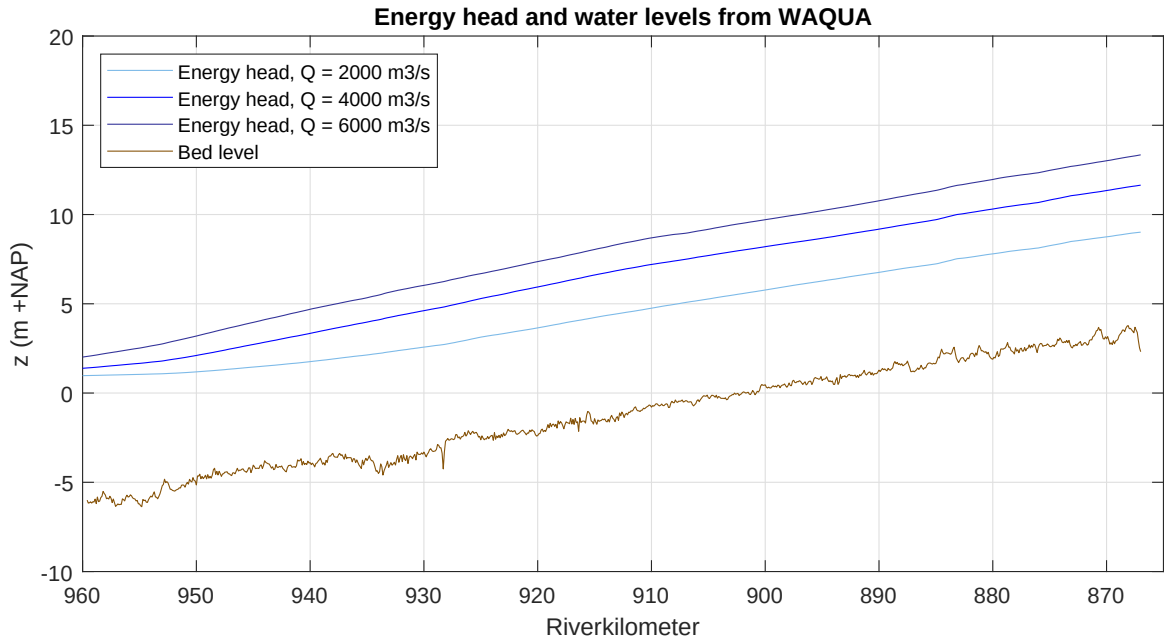

Figure 3.9: Energy head values for three discharges and bed level values from WAQUA simulations.

km at the upstream and downstream end of the river Waal. This is not a problem, since the identified normal flow segment does not extend to these river reaches.

To calculate the friction slope from the 1D energy head levels, only the second and third step of the processing steps used for the bed slope are applied. The first step, applying moving average before the slope is calculated, is not necessary because the energy head levels are already quite smooth (Figure 3.9). Similarly to the bed levels, the friction slope is calculated every kilometer by using a linear fit to all energy head values within that kilometer. In the third step, the friction slopes are averaged every 5 km to minimize the effect of possible outliers. The resulting bed slope and friction slopes are shown in Figure 3.10.

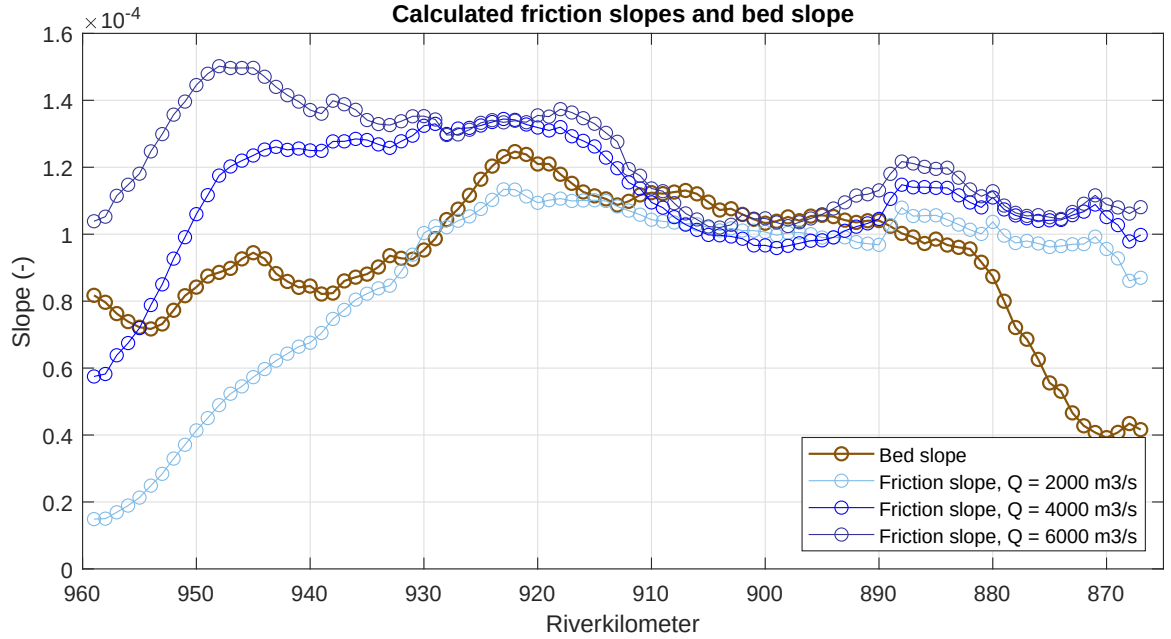

Figure 3.10: Friction slopes for three discharges and the bed slope derived from WAQUA simulations.

The lower friction slopes for Q = 2000 m^3/s and Q = 4000 m^3/s at the downstream reach of the river Waal correspond to the backwater curves in Figure 3.9. The friction slopes for Q = 4000 m^3/s and Q = 6000 m^3/s are a bit steeper in most of the backwater reach, between rkm 920 and rkm 950, than in the remainder of the river Waal. The friction slopes upstream of rkm 910 are approximately constant between $1.0 \cdot 10^{-4}$ and $1.2 \cdot 10^{-4}$. The wiggles of the friction slopes in the most upstream part of the river Waal, between rkm 867 and rkm 872, can be attributed to the less representative values due to the applied moving average. The bed slope shows large-scale wiggles, in the order of 5 km, at the downstream reach, which correspond to the bed elevation patterns in that area in Figure 3.9. The bed slope is approximately constant in the normal flow segment, from rkm 885 to rkm 920, with an average value between $1.0 \cdot 10^{-4}$ and $1.2 \cdot 10^{-4}$. In the most upstream part of the river Waal, between rkm 867 and rkm 885, the bed slope is much milder. This can partly be attributed to some flattening of the bed elevations in Figure 3.9, but we also assume that it is caused by the less representative values due to the applied moving averages. These less representative values extend over an area of 15 km, and have therefore a larger impact on the bed slope than on the friction slopes.

The relative difference from equation 3.2 is calculated with the bed and friction slopes from Figure 3.10, the result is indicated in Figure 3.11. As expected, the relative difference is lowest in the identified normal flow segment, between rkm 885 and rkm 920. The area between rkm 910 and rkm 930, that was previously indicated as possible border separating the normal flow and backwater segments, appears to be a transition zone between these segments, due to the relatively high wiggles in the relative slope difference. The highest relative difference that occurs within the identified normal flow segment, between rkm 885 and 920, for all three discharges combined is approximately 20%. The normal flow criterion is therefore 20%.

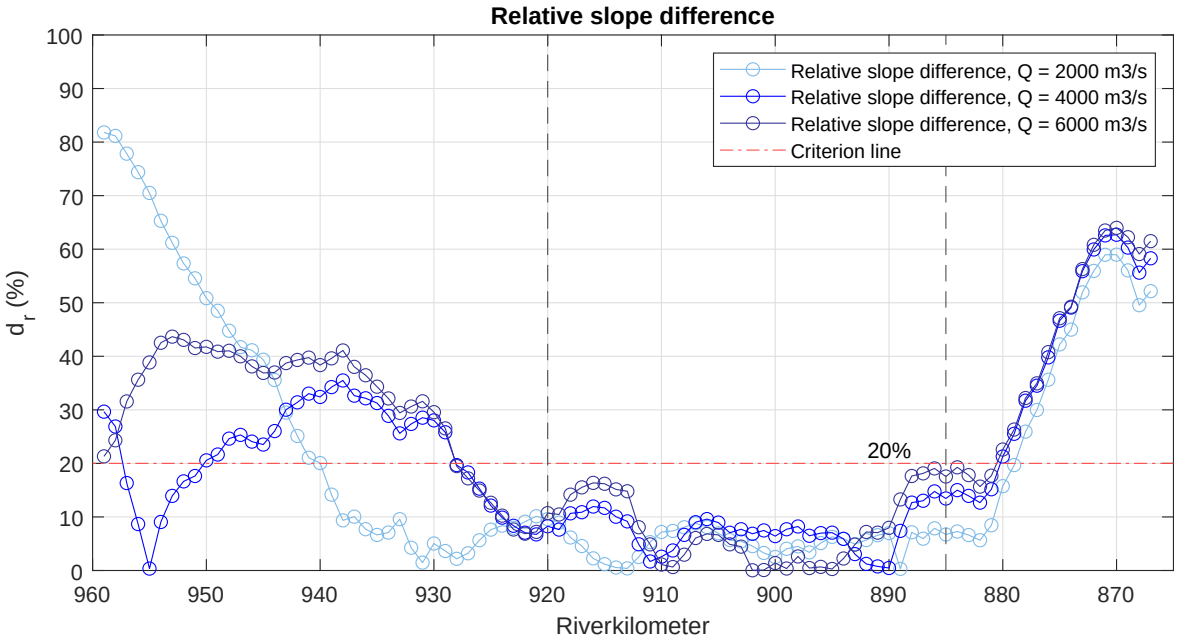

Figure 3.11: Relative slope difference for three discharges. The criterion is indicated with the red dash-dotted line.

It should be noted however that the approach to find this criterion has substantial uncertainties. The choice of which moving average values suit the approach best depends on the available data, and the criterion value varies strongly with the chosen moving averages. A criterion value of 1.5 to 2 times the current value is possible for lower moving averages that still result in seemingly representative bed and friction slopes. We therefore recommend to only use the criterion value of 20% as a first indication to identify a normal flow segment. Furthermore, we recommend to focus on the spatial differences of the relative slope difference, and to indicate a normal flow segment based on areas where this difference is consistently relatively low.

3.4. Measured bed slope

The bed slope that is representative for the state of the river Waal before the year 2014 is based on the temporally and spatially averaged biweekly multi-beam measurements of the bed elevation as presented in Section 3.3. To calculate the bed slope corresponding to these bed elevations, the same three processing steps as for the conversion of the modelled WAQUA bed levels are used; first a moving average of 20 km is applied to smooth the bed elevations, subsequently the bed slope is calculated using a linear fit per kilometer, and finally a moving average of 10 km is applied to reduce possible outlier influence. The measured bed slope is presented in Figure 3.12.

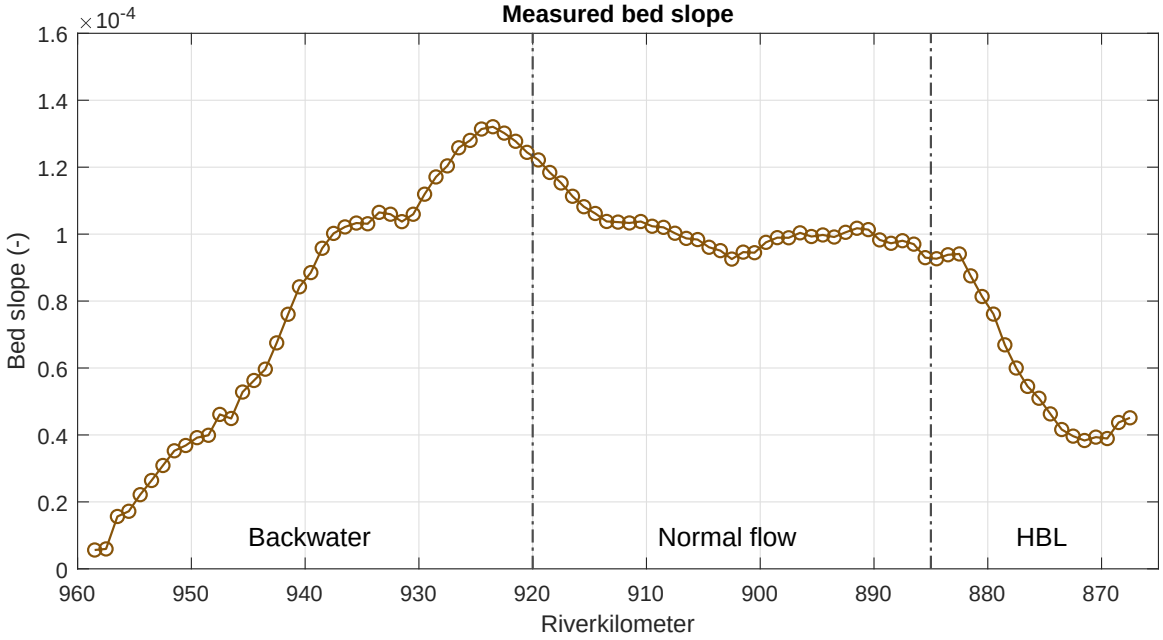

Figure 3.12: Measured bed slope of the river Waal from multibeam measurements.

The reason that the WAQUA bed levels are not used, is because we prefer direct measurements over modelled bed levels. We expect however that the bed slope calculated with bed levels from WAQUA are similar to the measured bed slope, because the bed level measurements form a basis for the modelled bed levels in WAQUA. If we compare the measured bed slope in Figure 3.12 with the WAQUA bed slope in Figure 3.10, it appears that they are approximately equal in the HBL. In the normal flow segment, they follow the same patterns, but the measured bed slope is about $0.1 \cdot 10^{-4}$ milder than the WAQUA bed slope. In the most upstream part of the backwater segment, between rkm 920 and rkm 940, the measured bed slope is approximately $0.1 \cdot 10^{-4}$ steeper, while in the most downstream part, between rkm 940 and rkm 960, the measured bed slope is much milder than the WAQUA bed slopes, with a maximum difference of $0.8 \cdot 10^{-4}$. These differences are conform the bed level measurements in Figure 3.7 and the WAQUA bed levels in Figure 3.9, but it is not known what the cause is of these bed level differences. Even though this downstream area has a mismatch between the measurements and WAQUA simulations, the bed slopes in the normal flow segment are quite similar. We therefore assume that using the measured bed slope does not lead to very different results from using the WAQUA bed slopes in the remainder of this research.

There are of course uncertainties related to the measured bed slope. It is outside the scope of this study to analyse what the bandwidth of uncertainties is. However, to give an impression of the order of magnitude of the uncertainties, the largest sources of uncertainty are identified.

The error of the bed elevation measurements is estimated to be between 0.05 m and 0.1 m (Ylla Arbós et al., 2020). The uncertainty that is caused by the processing steps to calculate the bed slopes is more difficult to define. It is assumed that the first processing step, the application of a moving average to the bed level measurements, results in the largest uncertainty. To get a feeling for the influence of this first step on the

uncertainty of the bed slope, this processing steps are repeated with a moving average of 8 km and 12 km respectively. The difference between the bed slopes identified in the normal flow segment in Figure 3.12 and the corresponding bed slopes using a moving average of 8 km and 12 km is at most $0.1 \cdot 10^{-4}$.

3.5. Measured bed surface sediment composition

To find the representative bed surface sediment composition of the river Waal, measurements of the bed surface sediment composition from the year 2020 (data courtesy: Rijkswaterstaat) are analysed. This measurement campaign has measured the bed surface sediment composition at three locations in the cross-section for every kilometer along the river Waal. We have grouped the measurements into six sediment fractions as indicated in Table 3.1. To visualize the bed surface sediment composition along the river Waal, first all fractions are cross-sectionally averaged over the three locations and subsequently a moving average of 10 km in longitudinal direction is applied to show the large-scale spatial trends. For consistency, only those kilometers are included where measurements of all three locations in the cross-section are available. The six bed surface sediment fractions are given in Figure 3.13. The gaps in the measured bed surface sediment fractions where no information is given, coincide with the non-erodible layers. Due to these river bed interventions, there is presumably either no sediment at these locations or it is too difficult to measure it. Even though the non-erodible layers do not span the entire width of the river, the bed surface sediment fractions are not given because there is not enough information along these cross-sections.

Table 3.1: Diameter ranges of the considered sediment fractions

Sediment fraction	Diameter range
Silt	< 63 μm
Fine sand	63 - 125 μm
Moderately fine sand	125 - 250 μm
Moderately coarse sand	250 - 500 μm
Coarse - very coarse sand	500 - 2000 μm
Gravel	> 2000 μm

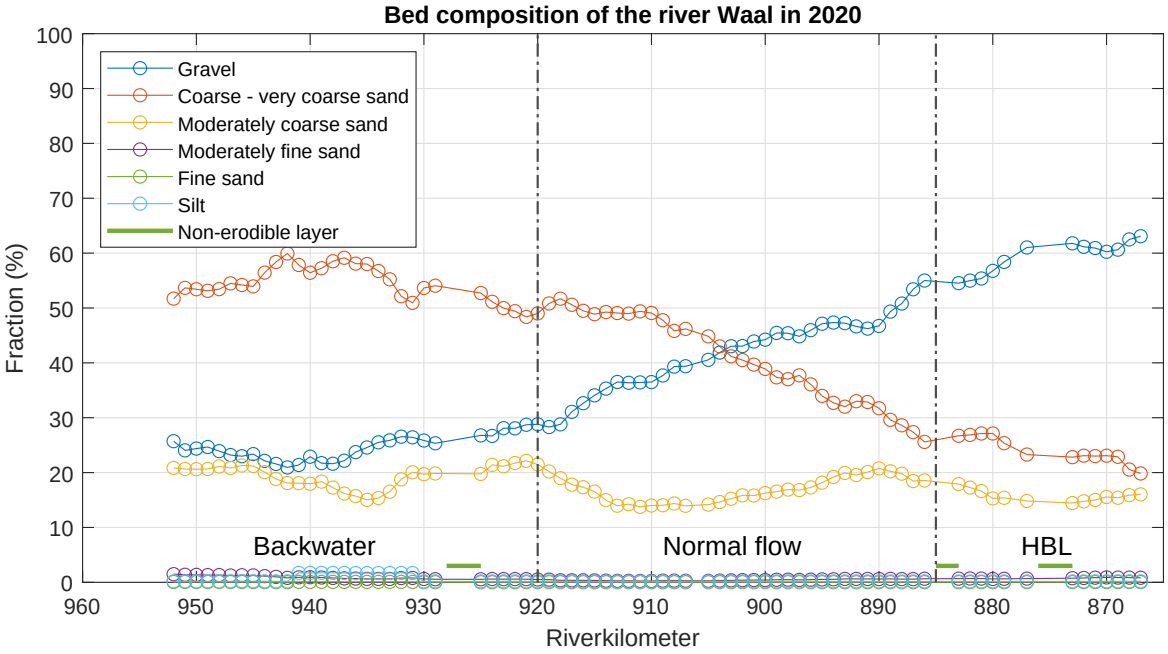

Figure 3.13: Measured bed surface sediment composition for six fractions in the year 2020. The non-erodible layers are marked in green.

It can be observed in Figure 3.13 that the three bed surface sediment fractions with the smallest diameters, silt, fine sand and moderately fine sand, are small compared to the other three fractions. These fractions are therefore not included in the representative description of the bed surface sediment composition of the river Waal. For simplicity, we combine the moderately coarse sand and coarse to very coarse sand fractions. This combined fraction is called the sand fraction in the remainder of this research, and consists of sediment particles with a diameter between 0.25 mm and 2 mm. The representative measured bed surface sediment composition therefore exists of a sand and gravel fraction, as shown in Figure 3.14. The bed surface sediment composition exists of mostly gravel in the upstream reach of the river Waal. The turning point, where more sand than gravel is found on the river bed, is approximately at rkm 890. Downstream from this turning point, the sand fraction is larger than the gravel fraction.

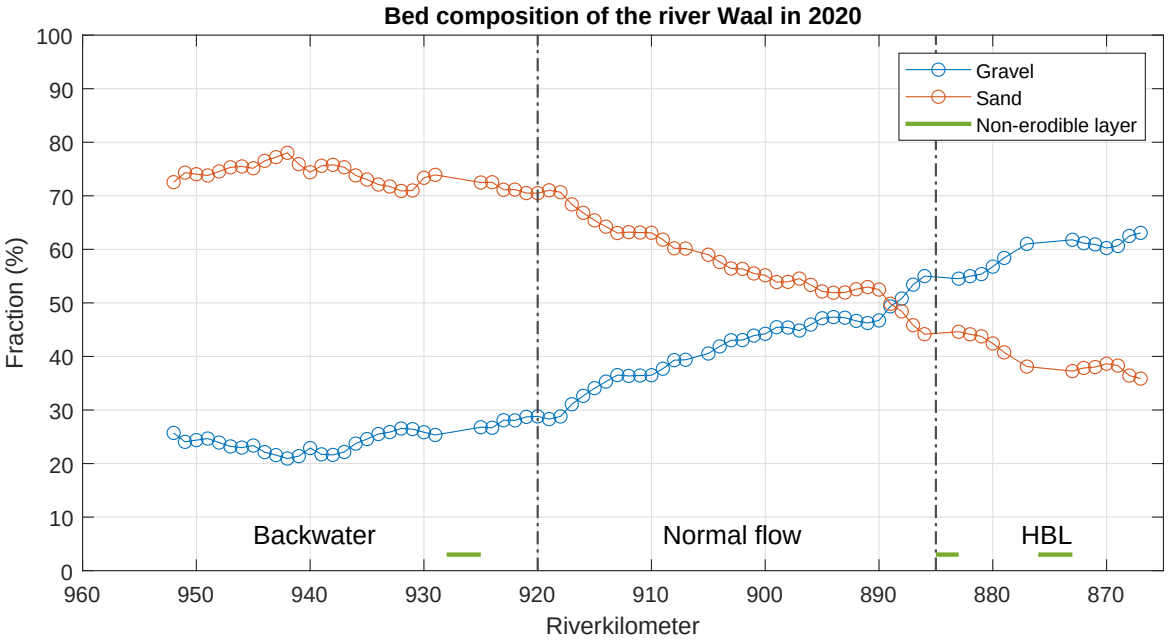

Figure 3.14: Measured bed surface sediment composition for the sand and gravel fractions for the year 2020. The non-erodible layers are marked in green.

Because the measurements used in this analysis are from the year 2020, and we are interested in the year 2014, we have also looked at the measured bed surface sediment composition of the year 1995 as described by Ten Brinke (1997). In those measurements, it is also clear that the three bed surface sediment fractions with the smallest diameters are negligible. Furthermore, similar to the measurements from the year 2020, the bed surface gravel fraction is larger at the upstream part and smaller at the downstream part of the river Waal than the bed surface sand fraction. Because the measurements of the years 1995 and 2020 are similar for these topics, we assume that the bed surface sediment composition measurements from 2020 are representative for the year 2014.

Similarly to the measured bed slope, it is outside the scope of this study to assess the uncertainty bandwidth related to the measured bed surface sediment composition, however an impression of the uncertainty sources is given here. According to Ylla Arbós et al. (2020), the uncertainty related to the measured grain size data is high because of a large variability in space and time and due to limited sampling density. It is assumed that the uncertainties related to the applied moving average are not larger than the measurement uncertainties.

4

Analytical relations and analyses approach

In this chapter, the analytical relations by Blom et al. (2017) are examined based on their applicability on the river Waal in Section 4.1 and they are used as a basis for a model to calculate equilibrium states. How the model works is explained in Section 4.2. Three different analyses are performed with this model; a deterministic analysis that results in a spatially varying equilibrium state without uncertainties, a sensitivity analysis that assesses the influence of each input parameter on the equilibrium state, and an uncertainty analysis that results in a bandwidth of possible equilibrium states. Their approach and input parameter values are explained in respectively Section 4.3, Section 4.4 and Section 4.5.

4.1. Assumptions and limitations of the analytical relations

Before the analytical relations by Blom et al. (2017) are applied to predict the equilibrium state of the river Waal, we investigate the influence of their assumptions and limitations on the case study. This is done by first identifying the assumptions and limitations, and subsequently assessing their effect on this study. One limitation and six assumptions are discussed in total.

An important limitation of the analytical relations by Blom et al. (2017) is that they are only applicable to normal flow segments. It is unknown how well these relations can predict an equilibrium state in an HBL or backwater segment, and it is thus preferable to only use them on normal flow segments. The consequence for the case study is that only normal flow segments of the river Waal can be included. The normal flow segment of the river Waal is identified in Section 3.3.

From all assumptions that are mentioned by Blom et al. (2017) in relation to the analytical relations, the most important ones for this study are: 1) there is no distinction between the main channel and the floodplains of a river, which means that the supplied water discharge remains in the main channel; 2) it is assumed that the hydraulic radius equals the flow depth, which implies that the channel width is relatively wide with respect to the flow depth; 3) the channel cross-sections are assumed to be rectangular; 4) it is assumed that the friction coefficient c_f (-) is independent of the bed surface texture and local flow parameters; 5) subsidence and uplift are neglected; and 6) there is only one grain size per sediment fraction entering the river upstream.

The consequences these assumptions have on the case study is discussed in the same order as the list of assumptions: 1) the distinction between the main channel and floodplains of the river Waal is very important, because large water volumes leave the main channel during higher discharges. If this distinction is not included in the equilibrium calculations, the amount of discharge is largely overestimated, which leads to different equilibrium state predictions. The assumption that there are no floodplains can thus not be made. To omit this problem, the fraction of water that remains in the main channel as a function of the discharge is included in the calculations.

2) The hydraulic radius and the flow depth depend on the discharge, which makes it difficult to assess whether the hydraulic radius and the flow depth are equal for all discharges. To create a general impression, the hydraulic radius is compared to the flow depth during the mean discharge of 2200 m^3/s at Lobith. The water depth is approximately 6 m for this discharge in the normal flow segment of the river Waal. This results in a hydraulic radius between 5.5 m and 6 m for a range of widths of the river Waal. The hydraulic radius is thus approximately equal to the flow depth for the mean discharge event. It is assumed that they are also approximately equal for the discharges that occur often in the river Waal, which means that this second assumption gives no problems for the equilibrium state calculations.

3) The cross-section of the river Waal is not perfectly rectangular, which might lead to a different equilibrium state prediction. However, we assume that the possible difference in equilibrium state due to another cross-sectional shape is negligible when compared to for example the equilibrium state differences due to uncertainties in the sediment transport values. It is therefore expected that this assumption does not have large consequences for this research.

4) The assumption that the friction coefficient is independent of the bed surface texture and local flow parameters is very likely not true. However, it is already difficult to determine a friction coefficient without taking bed surface texture and local flow parameters into account. We assume that including dependencies would be a better representation of the friction coefficient, however it would contribute to more uncertainty as well. It is not known how feasible it is to include dependencies, and whether it leads to more trustworthy equilibrium state predictions. The assumption that the friction coefficient is independent of the bed surface texture and local flow parameters is therefore adopted, but more research on the dependencies of the friction coefficient is recommended.

5) In this research, the equilibrium state of the river Waal is predicted for river control values that correspond to the year 2014. This means that no changes in time related to subsidence or uplift are included. Furthermore, if subsidence or uplift would occur, but slowly with respect to the timescale of the river response, the river will move towards a quasi-equilibrium state for which the analytical relations can be applied (Figure 2.1; Blom et al., 2017). The consequence of the assumption that the river Waal experiences no subsidence and uplift is thus assumed to be limited.

6) We have identified in Section 3.5 that the bed surface sediment composition exists of mainly sand and gravel. If we assume that only these two fractions enter the river Waal upstream, then all gravel particles entering the river have the same grain size and all sand particles have the same grain size. But in reality, a whole range of grain sizes enters the river Waal. This means that the analytical relations cannot represent all grain sizes entering the river upstream, unless more sediment fractions are described. However, the sediment supply and grain size data are very uncertain. We assume therefore that equilibrium state predictions including more sediment fractions have a similar uncertainty related to sediment supply and grain sizes as equilibrium state predictions with two sediment fractions. We expect thus that the assumption that there is only one grain size per sediment fraction at the upstream end of the river Waal has no negative consequences on the equilibrium state predictions.

In conclusion, most of the assumptions of the analytical relations by Blom et al. (2017) mentioned in this section are not expected to have a large influence on the equilibrium state predictions of the river Waal. There are however three components where extra attention is recommended. The first is that the water exchange between the main channel and floodplains is not included in the relations. Due to the expected large impact of this assumption, a workaround is invented that simulates the effect of the floodplains. The second component is the limitation that the analytical relations are only applicable to the normal flow segment. To be able to apply the analytical relations, the normal flow segment of the river Waal is identified. The last component is the assumption that the friction coefficient is independent of the bed surface sediment composition and local flow parameters, which is likely not true. Because it is not known whether the inclusion of dependencies would make the equilibrium state predictions better, this assumption is adopted. It is however recommended to study the impact of the dependencies of the friction coefficient on the equilibrium state calculations.

4.2. Model description

In this section a model is created with the analytical relations by Blom et al. (2017) that predicts the equilibrium state of the river Waal. This state consists of the bed slope i_b (-) and bed surface sediment composition. Because we have identified in Section 3.5 that the river Waal consists mostly out of sand and gravel, the model calculates the bed surface fractions of sand F_s and gravel F_g. Since the model uses only these two fractions, the bed surface gravel fraction is given by 100% minus the bed surface sand fraction and vice versa.

The model is based on the definition that the equilibrium bed slope is that slope for which the sediment transport is equal to the sediment supply upstream of a river. The general working method of the model is illustrated in Figure 4.1; the sediment transport is calculated in the model using the analytical relations and the model input parameters, and it is subsequently compared to measurements of the sediment supply at the upstream end of the river. If the sediment transport and supply values do not match, an iteration starts where the model chooses a new bed slope and bed surface sediment fractions to calculate the sediment transport again. This iteration continues until the sediment transport and supply values are equal. The bed slope and bed surface sediment fractions that were used for that calculation are the equilibrium values that form the model output.

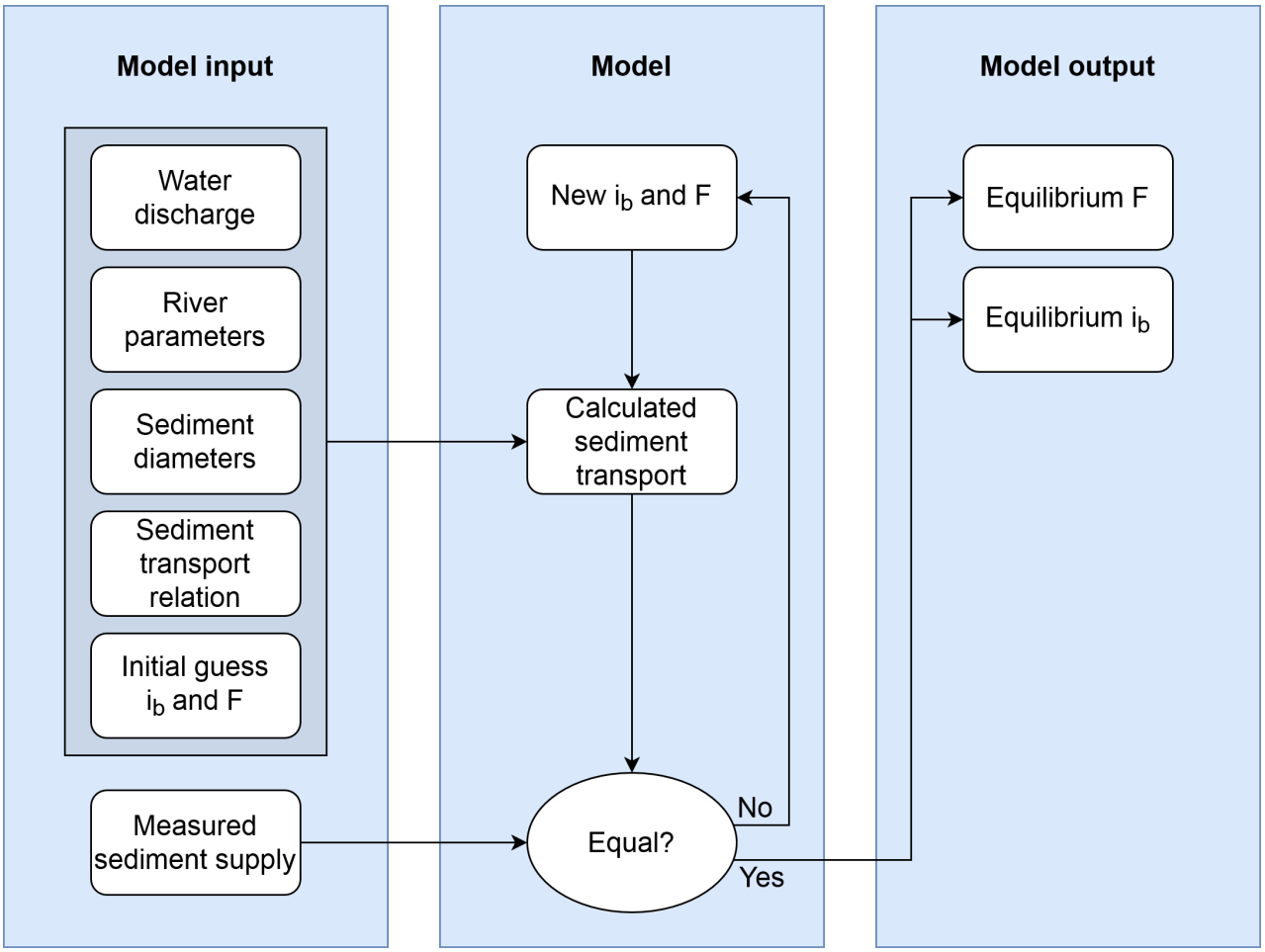

Figure 4.1: An overview of the model. i_b stands for bed slope and F for bed surface sediment fraction.

4.3. Deterministic analysis

In this section, the approach to calculate the deterministic equilibrium state is explained and the required input parameter values are given.

This deterministic analysis uses average parameter values as input for the model simulation. Spatial variation

of the parameters is included if this information is known, and otherwise a spatially constant average value is used. The resulting deterministic equilibrium state represents a spatially varying bed slope and bed surface sand fraction without uncertainties. The model is applied every 100 m along the river Waal, which means that every 100 m an equilibrium bed slope and an equilibrium bed surface sediment fraction is calculated.

The input parameters that the model requires are as indicated in Figure 4.1; water discharge Q (m^3/s), the river parameters width B (m) and friction coefficient c_f (-), diameters of sand D_s (mm) and gravel D_g (mm), measured sediment supply Q_s (m^3/s) for both the sand and gravel fraction, a sediment transport relation and an initial guess for the bed slope and bed surface sediment fractions. The parameter values that are used for the deterministic analysis are explained in this order.

The available water discharge is preprocessed before it is used in the model calculations. The preprocessing exists of three steps to create representative values for the main channel of the river Waal. The available water discharge data is a hydrograph at Lobith with daily measurements between the years 1901 and 2013 shown in Figure 4.2 (data courtesy: Rijkswaterstaat, data obtained from the Global Runoff Data Centre). The first step is to calculate how much of this water discharge from the river Bovenrijn enters the river Waal (Figure 3.2). As mentioned in Section 3.1, this discharge distribution is approximately 2/3 of the total discharge. However, for the model a more detailed discharge distribution is used that depends on the magnitude of the discharge in the Bovenrijn (Figure 4.3); a higher percentage of the water discharge enters the river Waal during low discharges than during high discharges at Lobith. There are however no agreements over the exact distribution values, which means that values in Figure 4.3 are an approximation (Reeze et al., 2015). After this step, the hydrograph contains water discharge values that enter the river Waal without taking floodplains into account.

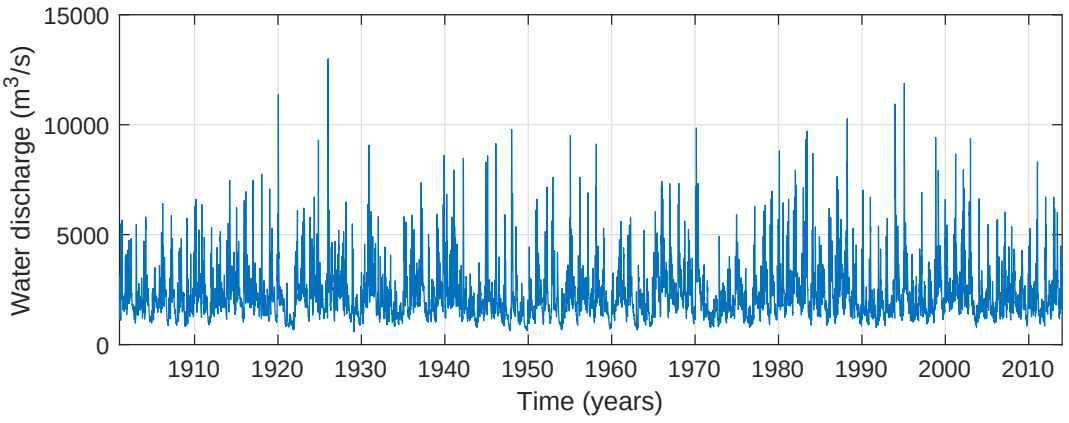

Figure 4.2: Hydrograph at Lobith for the years between 1901 and 2013.

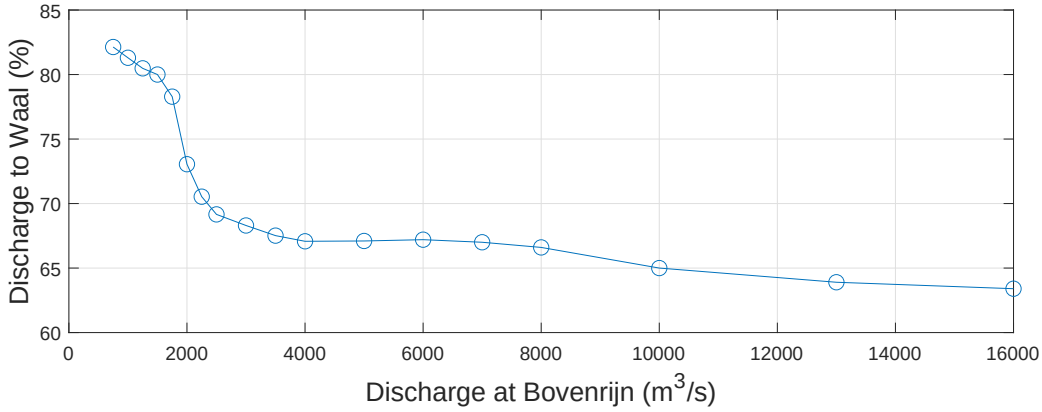

Figure 4.3: Water discharge distribution from the river Bovenrijn to the river Waal (data from Reeze et al. (2015)).

The second water discharge preprocessing step is to transform the hydrograph into a probability density function (PDF), which indicates the chance that a certain discharge will occur. Using a PDF reduces the computation time of the model, because every unique discharge value is only accounted for once, instead of accounting for every discharge value of the entire hydrograph. The PDF of the water discharges entering the river Waal is given in Figure 4.4.

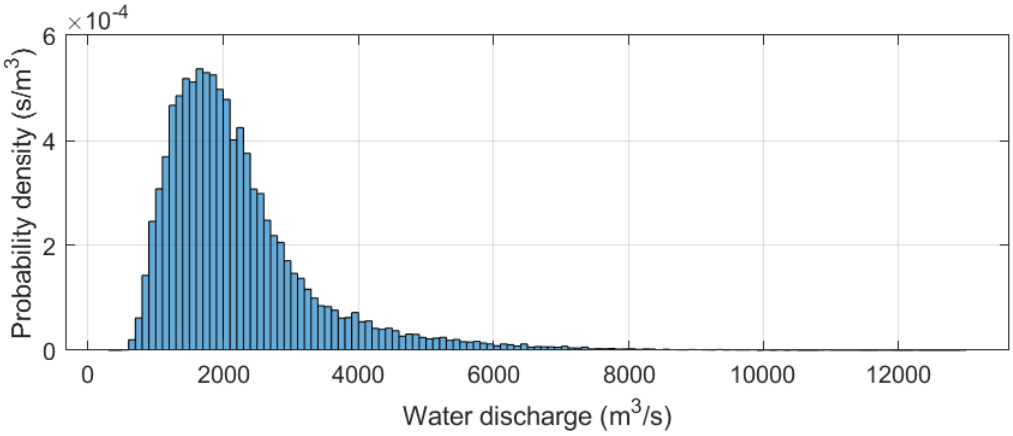

Figure 4.4: PDF at Lobith.

The third step compensates for the limitation of the analytical relations that there is no distinction between the main channel and the floodplains of a river. The PDF is multiplied by the fraction of the water discharge that remains in the main channel f_{Qmc} (-) as a function of the streamwise direction and the discharge magnitude. In this way, the water discharge that leaves the main channel towards the floodplains is subtracted from the water discharge that enters the river upstream, resulting in a PDF that represents the main channel of the river Waal. The water discharge fraction is computed using WAQUA simulations for five different discharges at Lobith, ranging from 2000 m^3/s to 10,000 m^3/s (Figure 4.5). These fractions should be values between zero and one, however some values are just above one. It is assumed that this is caused by rounding errors, and that the impact of these small errors is negligible. After these three processing steps, the water discharge of the main channel of the river Waal is represented by a PDF that varies in space.

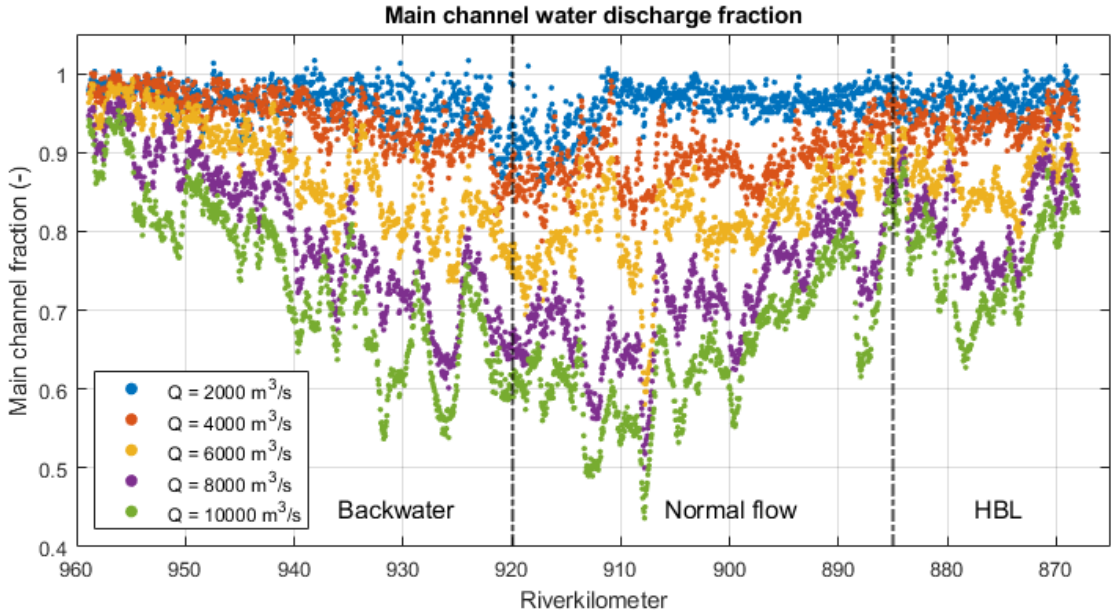

Figure 4.5: Main channel discharge fractions at the Waal as a function of water discharge at Lobith and space. The main channel discharge fractions are calculated with WAQUA simulations representing the year 2014.

The width of the main channel of the river Waal is assumed to be constant in time, since the Waal is an engineered river which means that the width is maintained. The width is however not constant in space, as can be seen in Figure 4.6. This spatial variability is included in the input of the model.

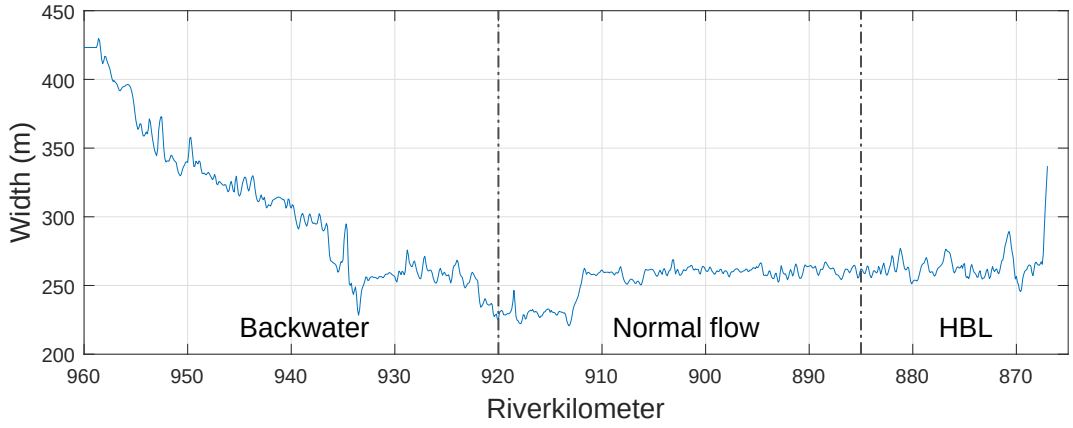

Figure 4.6: Main channel width of the river Waal.

The friction coefficient depends on various elements, such as bedforms, groynes and vegetation (e.g., Paarlberg et al., 2010). It is often used as a tuning parameter in numerical models to match the model simulation to measurements (e.g., Warmink, 2011), indicating that friction coefficient values are not well known. This, combined with the dependence on multiple elements, makes it difficult to determine the friction coefficient for this study. Determining this parameter by using for example measurements and existing relations is not within the scope of this study, as it could be an entire separate research. The friction coefficient is therefore based on literature, on the study by Van Vuren (2005). She uses a mean Chézy coefficient C ($m^{1/2}/s$) of the main channel of the river Waal of C = 40 $m^{1/2}/s$, which is $c_f = g/C^2$ = 0.0061. We have chosen to base the friction coefficient on this research, because it is an extensive study that also includes an uncertainty range that is required in the sensitivity analysis. However, the friction coefficient could have also been based on other research, such as for example on the studies by Warmink (2011) and Arkesteijn et al. (2019). This would have resulted in respectively a lower and higher friction coefficient. The impact that other friction coefficients have on the predicted equilibrium state and on the research questions is examined in the Discussion in Chapter 6.

The number of sediment fractions that are included in the model calculations is based on the analysis of the bed surface sediment composition in Section 3.5, where it was found that the bed surface of the river Waal consists mainly out of sand and gravel. These two bed surface sediment fractions are thus used in the model. For the model input an average diameter of the bed surface sand fraction D_s (mm) and of the bed surface gravel fraction D_g (mm) is needed. The choice of these average sediment diameters is based on the values that Rudolph (2018) and Blom et al. (2017) have used for calculations on the Dutch Rhine branches; 1 mm for the bed surface sand fraction and 10 mm for the bed surface gravel fraction. We assume that these average diameters are a good representation of the existent grain sizes within the two bed surface sediment fractions.

There are two sediment supply values required as input for the model; one value for the mean sand load $Q_{s0,sand}$ and one value for the mean gravel load $Q_{s0,gravel}$. These sediment supply values combined should represent the bed material load, which consists of the bed load and that part of the suspended load that interacts with the river bed (e.g., Rudolph 2018). The sediment supply values are based on the fractions above 2 mm in the sediment balance data by Frings et al. (2015). It is assumed that the sediment supply of the fractions below 2 mm in this sediment balance, the silt and clay particles, is suspended load that does not interact with the river bed, because all the mass that enters the river also leaves it again (Frings et al., 2015).

The sediment supply values upstream of the river Waal are not equal to the sediment transport values at the downstream end (Frings et al., 2015). This can be seen in Figure 3.5, where the total upstream sediment supply is 0.62 Mt/a, whereas the total sediment mass leaving the river Waal is 0.47 Mt/a. A pattern of more sediment mass entering than leaving the river Waal is also present when only the sand fraction is considered and similarly when only the gravel fraction is considered (Frings et al., 2015). This means that the sediment

transport varies along the river reach for both the sand fraction and the gravel fraction, which leads to a problem, because a river with a spatially varying sediment transport rate is very likely not in an equilibrium state (e.g., Buffington, 2012). Due to this problem, a choice must be made between two options to predict the equilibrium state of the river Waal that are both not satisfying. The first option is that the model predicts an equilibrium state with one average sediment supply value that does not fully represent the current state of the river. The second option is that the model uses spatially varying sediment transport values. These measured spatially varying values do represent the current state of the river, however we cannot assume that the bed slope and bed surface sediment fractions in the model output represent the equilibrium state of the river Waal.

The choice is made here to work with the first option that does not fully represent the state of the river Waal before the year 2014. The reason why is that the research questions are more focussed on predicting an equilibrium state than on representing the river Waal in the best way possible, and it is for this study also more valuable to perform a sensitivity and Monte Carlo analysis on an equilibrium state that is conform the definitions. If the measured upstream sediment supply is directly used in the model, then the sediment mass available in the river Waal would likely be overestimated, because in that case the mass loss along the river due to dredging and sedimentation on the floodplains is not taken into account (Figure 3.5). To reduce this problem, the average between the upstream sediment supply I_{up} and the sediment leaving the river Waal downstream O_{do} is used for the measured sediment supply Q_{s0} in the model:

$$Q_{s0} = \frac{I_{up} + O_{do}}{2} \tag{4.1}$$

The sediment supply values are based on the sediment budget study by Frings et al. (2015). In their research, no distinction is made between different sand classes, which means that the sand fraction consists of particles with diameters between 0.063 mm and 2 mm. The upstream sand supply is 0.56 Mt/a, and the downstream sand transport is 0.47 Mt/a, resulting in a mean sand load $Q_{s0,sand}$ of 0.51 Mt/a. There are two gravel classes given by Frings et al. (2015), one with particle diameters between 2 mm and 16 mm, and one with grain sizes between 16 mm and 63 mm. We combine the sediment transport values from these two classes, resulting in an upstream gravel supply of 0.07 Mt/a and in a downstream gravel transport of 0 Mt/a. The mean gravel load $Q_{s0,gravel}$ is thus 0.03 Mt/a. A sediment density of 2650 kg/m^3 is used to convert these sediment masses to sediment volumes.

There are four different sediment transport relations that are used in the model: Engelund and Hansen (1967), Ashida and Michiue (1972), Wilcock and Crowe (2003) and a generalized power law load relation (GR) with the same settings as used by Blom et al. (2017) (r = 0.05, $w_g = w_s = w = 0.4$ and c = 2.3). The equilibrium state is calculated for all four sediment transport relations.

The initial guesses for the river Waal are a bed slope of $i_b = 1 \cdot 10^{-3}$, a bed surface sand fraction of the sand supply divided by the total sediment supply, which is F_s = 0.94, and a bed surface gravel fraction of the gravel supply divided by the total sediment supply, which is F_g = 0.06. All three initial guesses are constant along the river reach.

4.4. Sensitivity analysis

This section explains how to calculate the sensitivity of the equilibrium state related to input value variations, which are caused by uncertainty or spatial differences. Furthermore, it shows which input parameter values are used, in the same order as in Section 4.3.

The aim of the sensitivity analysis is to identify how much influence input parameter variations have on the calculated equilibrium state of the river Waal. This helps to distinguish which parameters contribute most to the uncertainty in the equilibrium state predictions of the river Waal, and could for example be used in other studies to improve the model calculations. For this analysis, the uncertainty or spatial difference range of every model input parameter at the river Waal is investigated. Both the uncertainty and spatial differences are examined, because they both influence the equilibrium state, and it is interesting to investigate whether

the equilibrium state differences they cause is in the same order of magnitude. The uncertainty or spatial difference range is abbreviated to uncertainty range in this section. An uncertainty range of ten values is chosen for each input parameter that is expected to have influence on the calculated equilibrium state, and for each of these ranges a separate model simulation is performed. A constant average value is used for the other parameters. We have chosen to perform all sensitivity simulations on one location at the river Waal to focus on the differences between the parameters instead of on the effect that the uncertainty range has on various locations along the river. This means that the calculated equilibrium states do not vary spatially.

The water discharge can have uncertainties related to measurements and to its spatial variability. Uncertainties in measurements can be due to errors in a single measurement and due to inconsistencies in the measurement series. We estimate that the uncertainty due to errors of a single discharge measurement, which might be more than 100 m^3/s, is negligible with respect to the entire hydrograph. Next to that, we assume that there is no systematic under- or overestimation of the discharge. Variations of the water discharge due to measurement uncertainties are thus not included. There is uncertainty in the water discharge due to spatial variability in the fraction of water that remains in the main channel, which ranges from a fraction of 1 for the lowest discharges to a fraction of approximately 0.5 for the highest discharges (Figure 4.5). This variability is included in the sensitivity analysis by creating a range of ten values between the lowest and highest main channel discharge fraction as a function of the discharge.

It is possible that the measured width of the river Waal, as indicated in Figure 4.6, is not fully accurate. It is expected that variations of the river width are not larger than a few centimetres. The uncertainty of the river width is therefore much smaller than its spatial variability, which is in the order of tens of metres in the normal flow segment. The spatial variability of the width is therefore used as input for the sensitivity analysis, with a range of ten values between 200 m and 300 m. For the sensitivity analysis of the other parameters, a spatially average river width of the normal flow segment of 250 m is used.

The uncertainty range of the friction coefficient is based on the same thesis as the deterministic value of the friction coefficient for consistency. According to Van Vuren (2005), the coefficient of variation c_v (-) of the friction parameter is 0.15 and a lognormal distribution is a good representation. The mean value μ of the friction coefficient is 0.0061, which results in the distribution shown in Figure 4.7. From this distribution it appears that the smallest and largest possible friction coefficient values are respectively about 0.004 and 0.009. For the sensitivity analysis, ten values between 0.004 and 0.009 are used to represent the friction coefficient uncertainty.

The average sand and gravel diameter that were chosen in the deterministic analysis are respectively 1 mm and 10 mm. However, it is possible that other values better represent the sand and gravel fractions that enter the river Waal. To include this uncertainty in the sensitivity analysis, a range of possible sand and gravel diameters is identified. These ranges are calculated with a coefficient of variation of 0.07, which is an approximation based on the coefficients of variation that Van Vuren (2005) has computed for median grain sizes along the river Waal. Even though these coefficients are calculated for one fraction that contains all sediment diameters, we assume that they can also be used on the two sediment fractions that are considered in this research. Furthermore, a uniform distribution of the sediment grain sizes is assumed, which was also used by Van Vuren (2005). With a uniform distribution, an average diameter of 1 mm and a coefficient of variation of 0.07, the range of the sand diameter is between 0.88 mm and 1.1 mm. This seems to be a small range of uncertainty, especially since there are not many measurements or other sources of information that this range can be based on. A somewhat larger range of uncertainties is therefore used for the sand diameter, ranging from 0.8 mm to 1.2 mm. The same value of the coefficient of variation is applied on the average gravel diameter of 10 mm, resulting in a gravel diameter range between 8.8 mm and 11 mm. Also for the gravel fraction a larger range is chosen due to the lack of information, ranging from 8 mm to 12 mm. Ten values within the ranges of both the sand and gravel diameters are used in the sensitivity analysis.

There are two types of uncertainties that play an important role for the sediment supply. The first type is the uncertainty of the total sediment supply along the river reach, and the second is the distribution of the gravel load with respect to the sand load. These uncertainties depend on the availability, quality, character and processing method of underlying data, and are typically in the order of 25 to 75% (Frings et al., 2019).

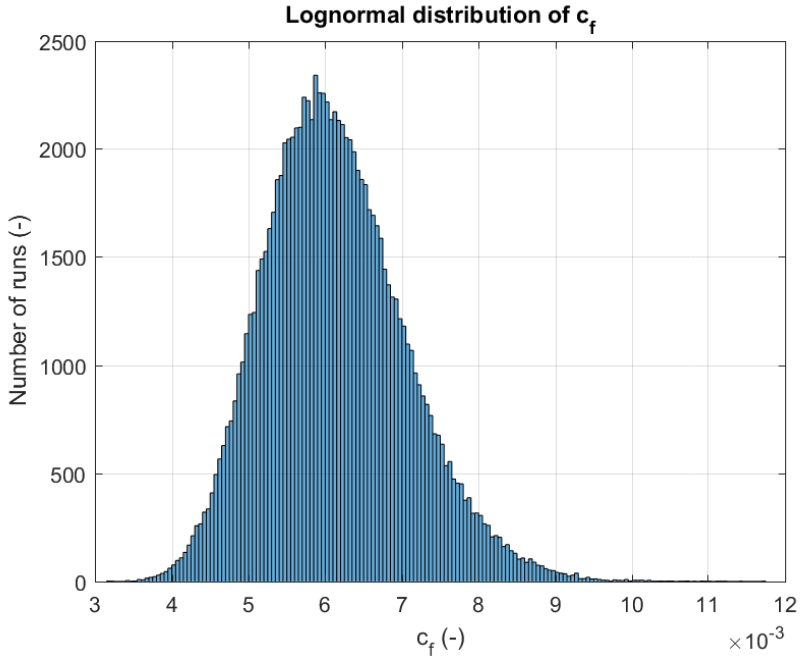

Figure 4.7: The lognormal distribution of the friction coefficient.

According to Frings et al. (2015), the uncertainty related to the total sediment supply is approximately 50% for both the upstream and downstream end of the river Waal. As discussed in the previous section, a spatially constant sediment supply is used to predict the equilibrium state. The average total sediment transport is the combination of the average sand and gravel transport given in the previous section, $Q_{s0,total}$ = $Q_{s0,sand}$ + $Q_{s0,gravel}$ = 0.55 Mt/a. Applying the 50% uncertainty to the sediment transport results in $Q_{s0,total} \pm 50\% \cdot Q_{s0,total}$ = 0.27 Mt/a and 0.82 Mt/a. For the sensitivity analysis, ten values between 0.27 Mt/a and 0.82 Mt/a are used, while maintaining the same ratio between the sand supply and the gravel supply as in the deterministic analysis.

The amount of gravel with respect to the amount of sand within a given total sediment supply value is also uncertain. In the deterministic calculation of the previous section, the distribution is $Q_{s0,gravel}/Q_{s0,total} \cdot 100\%$ = 6% gravel and thus 94% sand. According to Frings et al. (2015), the gravel supply has an uncertainty between 80% for the smaller gravel particles and 140% for the larger gravel particles. We have chosen to apply an uncertainty of 100% to the deterministic gravel supply, which leads to a possible mean gravel content of the total sediment supply p_g (-) between 0% and 12%. The sand supply value is the total sediment supply minus the gravel supply. For the sensitivity analysis, ten values between a gravel content of 0% to 12% are used.

The use of a certain sediment transport relation results in uncertainty, since these sediment transport relations are empirical and because none of them has a universal applicability (Fernández and Garcia, 2017). To reduce this uncertainty, four different sediment transport relations have been used in the deterministic runs. The sensitivity analysis is performed for these four sediment transport relations as well. No additional uncertainty related to the transport relations is considered here.

The initial guesses for the bed slope and bed surface sediment fractions do not contribute to uncertainty or sensitivity in the model outcome, because different guesses still lead to the same model outcome. The initial guesses only have influence on the duration of the model runs, and are not included in the sensitivity analysis.

The values that are used in the sensitivity analysis are presented in Table 4.1.

Table 4.1: The average values and uncertainty ranges that are used for the sensitivity analysis. For the main channel discharge fraction f_{Qmc}, the average value depends on the discharge, and the uncertainty range is between the lowest and highest main channel discharge fractions as a function of the discharge.

Input parameter	Symbol	Average	Uncertainty range	Unit
Main channel width	B	250	200 - 300	m
Friction coefficient	c_f	0.0061	0.004 - 0.009	-
Sand diameter	D_s	1	0.8 - 1.2	mm
Gravel diameter	D_g	10	8 - 12	mm
Total sediment transport	$Q_{s0,total}$	0.55	0.27 - 0.82	Mt/a
Mean gravel content of the sediment supply	p_g	6	0 - 12	%

4.5. Uncertainty analysis

In this section, the approach of the uncertainty analysis and the required model input are given.

An uncertainty analysis is performed to examine the range of possible equilibrium state predictions due to the uncertainties related to the input parameters. The desired result of this analysis is a bandwidth of possible equilibrium states of the river Waal that gives a 90% confidence interval, which means that there is a confidence of 90% that the equilibrium state for the given input parameters is within this bandwidth. To obtain a 90% confidence interval, a Monte Carlo simulation is applied where as many combinations of input parameter values as feasible are used to calculate possible equilibrium states. The value of an input parameter is either deterministic for all computations, or is randomly chosen according to a distribution that represents its uncertainty.

How many input parameters with uncertainty distributions are included in the Monte Carlo analysis depends on the balance between the reliability of the 90% confidence interval and the needed computation time. The reliability of the 90% confidence interval increases when more uncertainty distributions are included. However, the number of Monte Carlo simulations that is recommended to obtain a reliable 90% confidence interval is higher when the number of input parameters that have an uncertainty distribution is larger, leading to a longer computation time. To prevent long computation times, a compromise is made between the number of uncertainty distributions and the number of Monte Carlo simulations; it is chosen to perform 100,000 simulations with uncertainty distributions for three input parameters, and deterministic values for the remaining input parameters. This results in a computational time of approximately two hours for one location. Applying the Monte Carlo analysis every 100 m along the normal flow segment of the river Waal would result in a computation time of approximately one month, which is not feasible. It is therefore decided to perform the Monte Carlo analysis on one location that represents the normal flow segment of the river Waal. It is assumed that the resulting 90% confidence interval can be roughly applied to the spatial results of the deterministic analysis, to give an impression of the possible range of equilibrium states along the normal flow segment of the river Waal.

The three input parameters that have an uncertainty distribution in the Monte Carlo analysis are the ones for which the expected range of possible equilibrium states is the largest. Only distributions based on uncertainty of input parameters are included. Variations in input parameter values due to spatial differences are excluded, because the equilibrium state uncertainties are calculated for a certain location. If spatial variations would be included, the predicted equilibrium state range would be overestimated. The main channel width and main channel discharge fraction vary along the river Waal, and have thus no uncertainty distribution in the Monte Carlo analysis. Of the remaining input parameters, it is assumed that the friction coefficient, the total sediment transport and the mean gravel content in the total sediment transport lead to the largest range of possible equilibrium states due to their large uncertainties. This means that deterministic values are used for main channel width, the main channel discharge fraction, and the sand and gravel diameters. The main channel discharge fraction dependence on the discharge value in the hydrograph remains, but because the hydrograph is equal for each Monte Carlo simulation, there is no difference in main channel discharge fraction

between the simulations.

The lognormal distribution of the friction coefficient as presented in Section 4.4 (Figure 4.7), with a mean value of 0.0061, is used as an uncertainty distribution in the Monte Carlo analysis.

To identify an uncertainty distribution of the total sediment supply, it is assumed that the sediment supply follows a normal distribution. It is estimated that the edges of three times the standard deviation are approximately the 50% uncertainty values of the total sediment transport, which were identified in Section 4.4 as 0.27 Mt/a and 0.82 Mt/a. This results in a standard deviation of $\sigma = 0.09$ Mt/a. The normal distribution of the total sediment transport supply is shown in Figure 4.8.

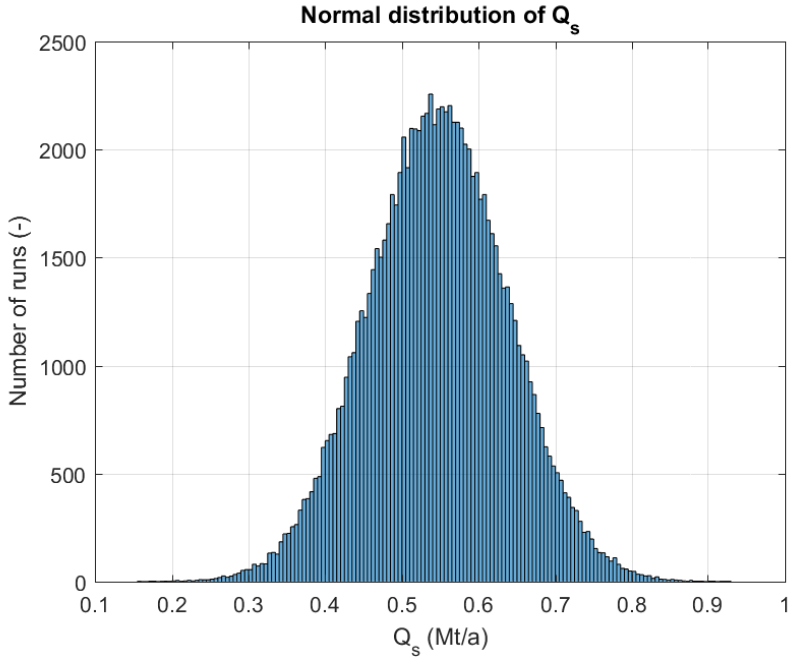

Figure 4.8: The normal distribution of the total sediment supply upstream of the river Waal.

For the uncertainty distribution of the mean gravel content of total sediment transport a uniform distribution is used with values between 0% and 12%, as indicated in Figure 4.9. A uniform distribution is chosen because the division of chances between the possible mean gravel content values is not known, which makes a distribution with an arbitrary outcome a suitable choice. It should be noted however that it is very unlikely that there is no mean gravel content in the total sediment supply, due to the observed coarsening of the sediment entering the river Waal (Figure 3.4). This implies that a uniform distribution likely results in a somewhat larger 90% confidence interval than a distribution where the chance that the mean gravel content is 0% would be lower than other mean gravel content values.

The bandwidth that follows from the Monte Carlo analysis gives an indication of the possible equilibrium states of the river Waal, and thus of the uncertainty in equilibrium state calculations due to uncertainty in the input parameters. However, not all uncertainties are represented, because only three uncertainty ranges of input parameters are included in this analysis. Furthermore, the identified uncertainty distributions are an approximation, there is no exact knowledge about the uncertainty ranges. This means that the calculated 90% confidence interval is an approximation and should only be used as a rough indication of the range of possible equilibrium states, which is sufficient for this research.

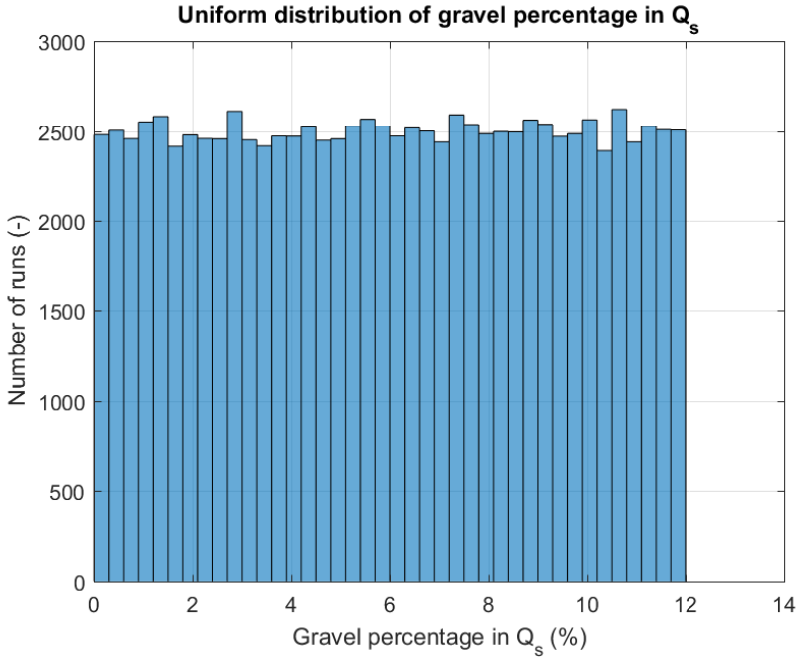

Figure 4.9: The uniform distribution of the gravel percentage of the total sediment supply.

5

Results equilibrium state calculations

This chapter presents the results from the deterministic analysis in Section 5.1, the sensitivity analysis in Section 5.2 and the uncertainty analysis in Section 5.3. The equilibrium state calculations are compared to the measured state of the river Waal in Section 5.4.

5.1. Results deterministic analysis

This section presents the results from the deterministic analysis as explained in Section 4.3. The results consist of spatially varying equilibrium bed slopes and spatially varying equilibrium bed surface sand fractions for the four sediment transport relations; Engelund and Hansen (1967) (EH), a generalized power law load relation (GR), Ashida and Michiue (1972) (AM), and Wilcock and Crowe (2003) (WC).

The predicted deterministic equilibrium bed slope of the normal flow segment of the river Waal is given in Figure 5.1. The predicted bed slope is at least $4.5 \cdot 10^{-5}$ and at most $7.5 \cdot 10^{-5}$. The average bed slope depends on the sediment transport relation, and is $6.2 \cdot 10^{-5}$ for EH, $7.0 \cdot 10^{-5}$ GR, $5.4 \cdot 10^{-5}$ for AM and $6.1 \cdot 10^{-5}$ for WC. This means that the bed slope differences between the load relations are at most a factor 1.3. The difference between the largest and smallest equilibrium bed slope within one sediment transport relation is between $0.9 \cdot 10^{-5}$ and $1.8 \cdot 10^{-5}$ for all four sediment transport relations.

When analysing the large scale patterns along the river Waal, the predicted bed slopes are approximately constant in space for all relations. However, the bed slope appears to be a bit larger at the centre of the normal flow segment between rkm 890 and rkm 910, especially for the AM sediment transport relation. Spatial differences in the equilibrium bed slope can only be caused by variations in the water discharge due to the varying main channel discharge fraction (Figure 4.5) and by variations in the main channel width (Figure 4.6). To investigate which of these two input parameters causes the bed slope to be larger in the middle of the normal flow segment, the deterministic equilibrium state is given as a function of only the variable width by ignoring the floodplains (Figure 5.2a), and as a function of only the variable water discharge by using a spatially constant width of 250 m (Figure 5.2b). From Figure 5.2, it appears that the influence of the variable width on the spatial differences in the equilibrium bed slope is small compared to the variable water discharge, expect for the small jump around rkm 912, which corresponds to the sudden smaller width (Figure 4.6). That the equilibrium bed slope is steeper in the middle of the normal flow segment appears to be caused by the varying water discharge due to the main channel discharge fraction. The equilibrium bed slope would have been even steeper in the most upstream region, which also corresponds to the global pattern of a lower main channel discharge fractions in downstream direction in Figure 4.5, if the width narrowing would not have worked as a counter effect.

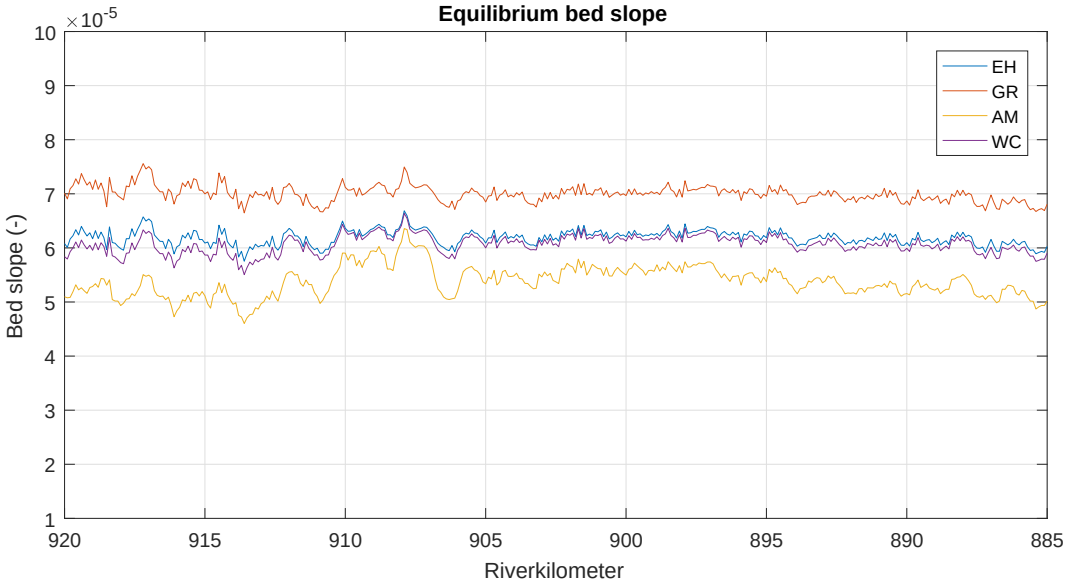

Figure 5.1: The predicted equilibrium bed slope from the deterministic analysis, based on the following sediment transport relations: Engelund and Hansen (1967) (EH), a generalized load relation (GR, where r = 0.05, $w_g = w_s = w$ = 0.4 and c = 2.3), Ashida and Michiue (1972) (AM) and Wilcock and Crowe (2003) (WC).

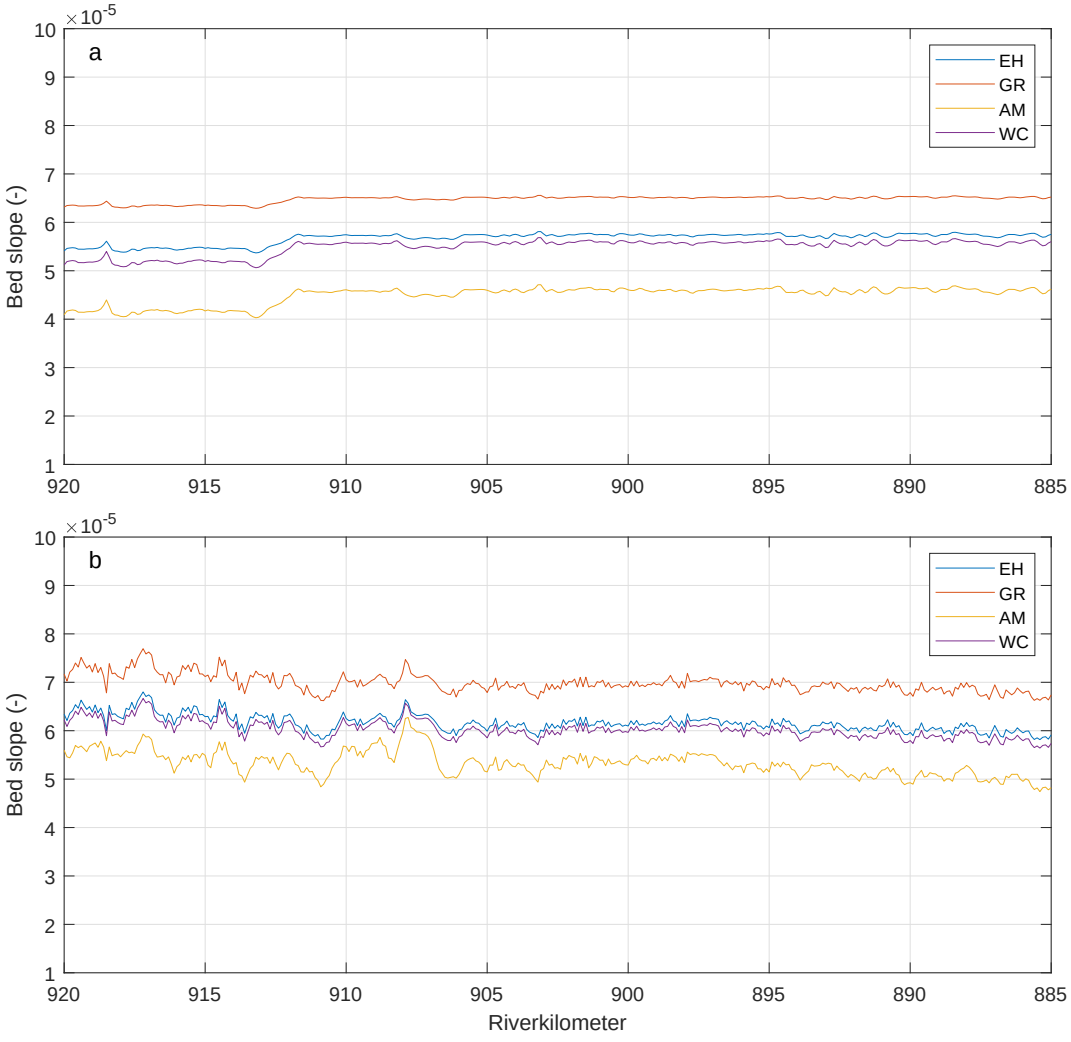

Figure 5.2: The deterministic equilibrium bed slope, where a) the spatial differences are only caused by the varying width because the main channel discharge fraction is not included and b) the spatial differences are only caused by the varying water discharge because the width is a spatially constant value of 250 m.

The wiggles that are visible in the equilibrium bed slope in Figure 5.1 are approximately the same for all four sediment transport relations. Their pattern appears to be mainly caused by the wiggles in the main channel discharge fraction, as can be deduced from Figure 5.2.

The predicted deterministic equilibrium bed surface sand fraction of the normal flow segment of the river Waal is given in Figure 5.3. For all transport relations, the equilibrium bed surface sand fraction is above 50%, which means that there is more sand than gravel present on the bed surface in the calculated equilibrium state. The average equilibrium bed surface sand fraction is 61% for EH, 87% for GR, 56% for AM and 66% for WC, which results in a maximum difference of approximately 30% between the sediment transport relations.

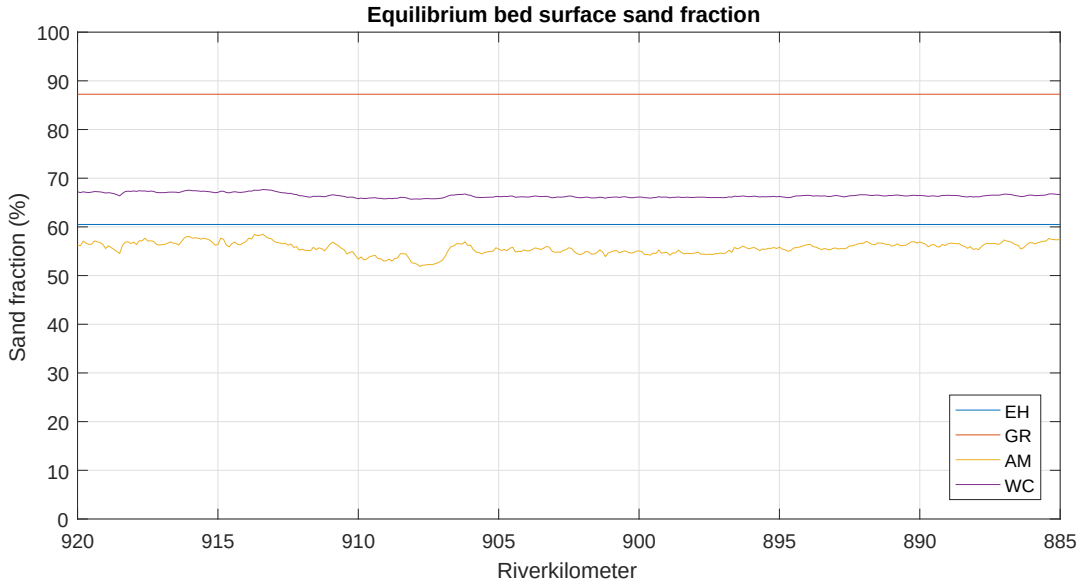

Figure 5.3: The predicted equilibrium bed surface sand fraction from the deterministic analysis, based on the following sediment transport relations: Engelund and Hansen (1967) (EH), a generalized load relation (GR, where r = 0.05, $w_g = w_s = w$ = 0.4 and c = 2.3), Ashida and Michiue (1972) (AM) and Wilcock and Crowe (2003) (WC).

The equilibrium bed surface sand fractions are constant in space for the EH and GR load relations, whereas the equilibrium bed surface sand fractions show wiggles for the AM and WC load relations. The reason that the bed surface sand fractions are spatially constant for the EH and GR load relations is because they are only a function of the sediment diameters and the mean gravel content of the total sediment supply, which are constant in the model. The equilibrium bed surface sand fractions calculated with the AM and WC load relations depend on the spatially varying main channel width and water discharge, which cause the wiggles along the normal flow segment. Similarly to the wiggles in the equilibrium bed slopes in Figure 5.1, the wiggles are mainly caused by the spatially varying water discharge due to the main channel discharge fractions (Figure 4.5). The sudden decrease in the main channel width around rkm 912 in downstream direction (Figure 4.6) leads to a small increase of the equilibrium bed surface sand fractions for the AM and WC load relations downstream of rkm 912.

5.2. Results sensitivity analysis

This section presents the results from the sensitivity analysis in Section 4.4. First the sensitivity of the equilibrium bed slope and subsequently the sensitivity of the equilibrium bed surface sand fractions on the input parameters are given. The input parameters that are included in this analysis are the main channel width B, the friction coefficient c_f, the sand diameter D_s, the gravel diameter D_g, the total sediment supply Q_s, the mean gravel content in the total sediment supply p_g and the main channel discharge fraction f_{Qmc}.

Figure 5.4 shows the results of the sensitivity analysis for the equilibrium bed slope for the seven selected input parameters. The minimum bed slope that follows from this analysis is $1 \cdot 10^{-5}$, and the maximum bed slope is $10 \cdot 10^{-5}$. All other calculated bed slopes in the sensitivity analysis are within this range.

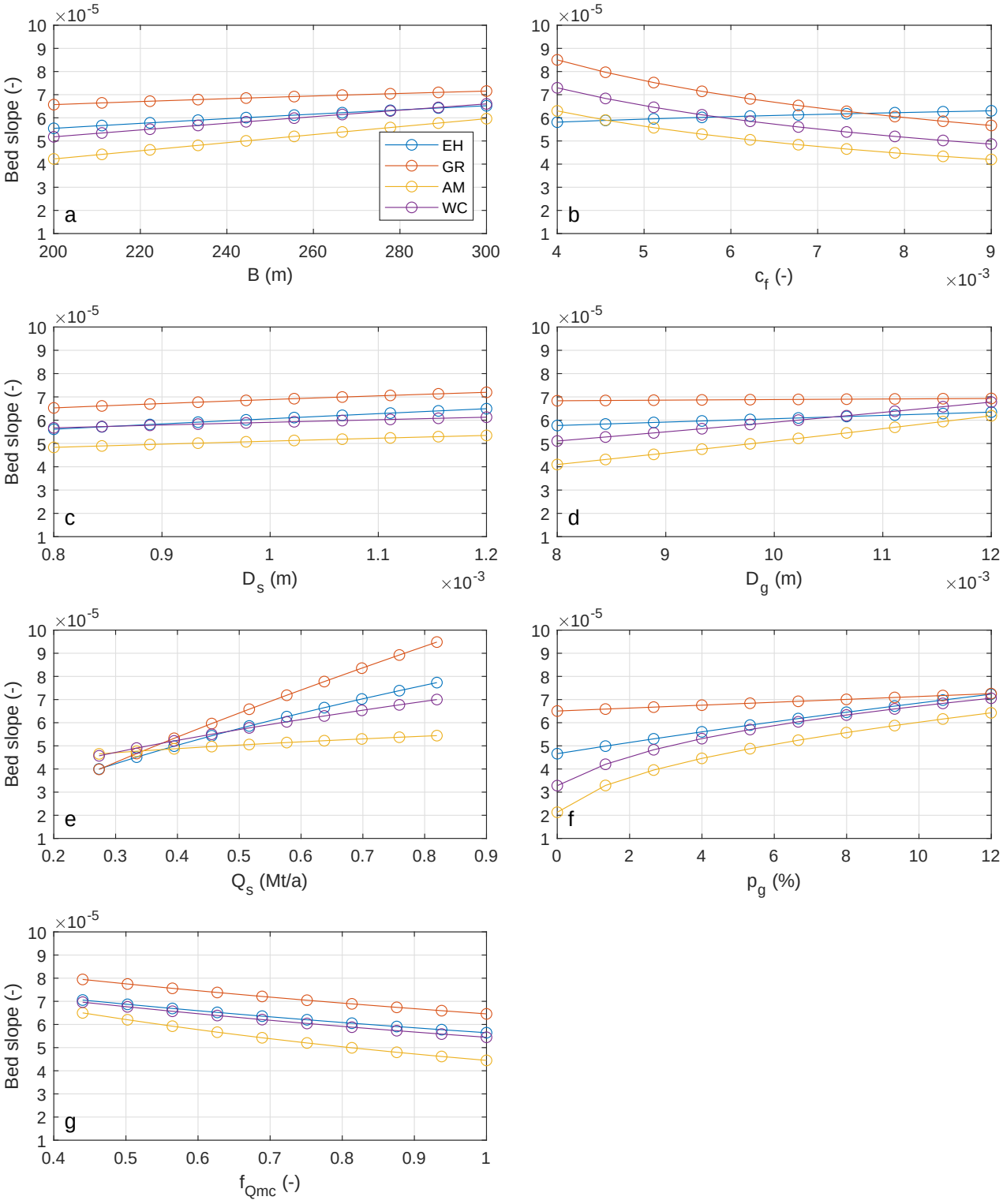

Figure 5.4: Sensitivity analysis of the equilibrium bed slope for a varying: (a) channel width, (b) friction coefficient, (c) sand diameter, (d) gravel diameter, (e) total sediment supply, (f) mean gravel content in total sediment supply and (g) main channel discharge fraction. The calculations are based on the Engelund and Hansen (1967) load relation (EH), the generalized load relation (GR, where r = 0.05, $w_g = w_s = w$ = 0.4 and c = 2.3), the Ashida and Michiue (1972) load relation (AM) and the Wilcock and Crowe (2003) load relation (WC).

To get an impression of which parameter ranges lead to the most sensitivity in the equilibrium bed slope, the bed slope difference between the largest and smallest parameter values is analysed per sediment transport relation. The parameter that results in the largest uncertainty in the calculated equilibrium bed slope, is the parameter for which the difference between the bed slopes is the largest. This is the case for the total sediment supply parameter when looking at the GR and EH load relations, and for the mean gravel content in the total sediment supply when looking at the AM and WC load relations. For these calculations the equilibrium bed slope difference is between $4 \cdot 10^{-5}$ and $5.5 \cdot 10^{-5}$, which is at least $1 \cdot 10^{-5}$ larger than the other equilibrium bed slope differences.

From the above observation it is clear that the parameters that have the most and the least impact on the outcome uncertainty of the model are not the same for all load relations. Each load relation has their own sequence of parameter impact, but the AM and WC load relations show some similarities, and the EH and GR load relations as well. For all parameters except the friction coefficient and the lowest sediment transport values, the GR load relation results in the highest average equilibrium bed slopes, the AM load relation in the lowest slopes and the EH and WC load relations result in approximately the same average slopes.

The sensitivity of the equilibrium bed slope due to spatial variations, represented by the main channel width and the main channel discharge fraction, is in the same order of magnitude as the sensitivity due to uncertainties, represented by the other input parameters. This means that a difference in the equilibrium bed slope between two locations is in the same order of magnitude as a difference in the equilibrium bed slope due to uncertainties of an input parameter.

For every parameter in Figure 5.4 except the friction coefficient, the influence of a larger parameter value on the equilibrium bed slope is unambiguous; the equilibrium bed slope increases for a larger main channel width, sand diameter, gravel diameter, total sediment supply and mean gravel content in the total sediment supply, and the bed slope decreases for a larger main channel discharge fraction. The effect of a larger friction coefficient is less clear, because the equilibrium bed slope increases for the EH load relation, but it decreases for the other load relations. Rudolph (2018) has used the same analytical relations as in this research, however she finds an increasing bed slope for an increasing friction coefficient for the WC load relation. We would therefore expect that for this load relations an increase in friction coefficient would lead to an increase in the equilibrium bed slope, which is opposite to the observations from Figure 5.4. This means that there is possibly something wrong in the model, however the cause has not been found.

Figure 5.5 shows the results of the sensitivity analysis for the equilibrium bed surface sand fraction. For every parameter and all four sediment transport relations, the calculated equilibrium bed surface sand fraction is somewhere between 40% and 100%.

It depends on which sediment transport relation is used whether a parameter has influence on the bed surface sand fraction. When the GR and EH load relations are used, the bed surface sand fraction remains constant for the width, the friction coefficient, the total sediment supply and the main channel discharge fraction. The bed surface sand fraction has a very small difference for the sand and gravel diameters for the GR load relation. The AM and WC load relations have influence on the bed surface sand fraction for every parameter except for the friction coefficient, although the influence of the WC load relation on the main channel discharge fraction is also very limited.

It is clearly visible from Figure 5.5 that the parameter that results in the largest bed surface sand fraction differences is the mean gravel content of the total sediment supply. The parameter that results in the largest sensitivity after the mean gravel content of the total sediment supply is less clear; it is either the total sediment supply or the gravel diameter for the AM and WC load relations, and either the sand diameter or the gravel diameter for the EH and GR load relations.

The sensitivity of the equilibrium bed surface sand fraction due to spatial variations, represented by the main channel width and the main channel discharge fraction, has a smaller order of magnitude than the sensitivity due to uncertainties, represented by the other input parameters. This means that a difference in the equilibrium bed surface sand fraction between two locations is generally speaking less significant than a difference in the equilibrium bed surface sand fraction due to uncertainties of an input parameter.

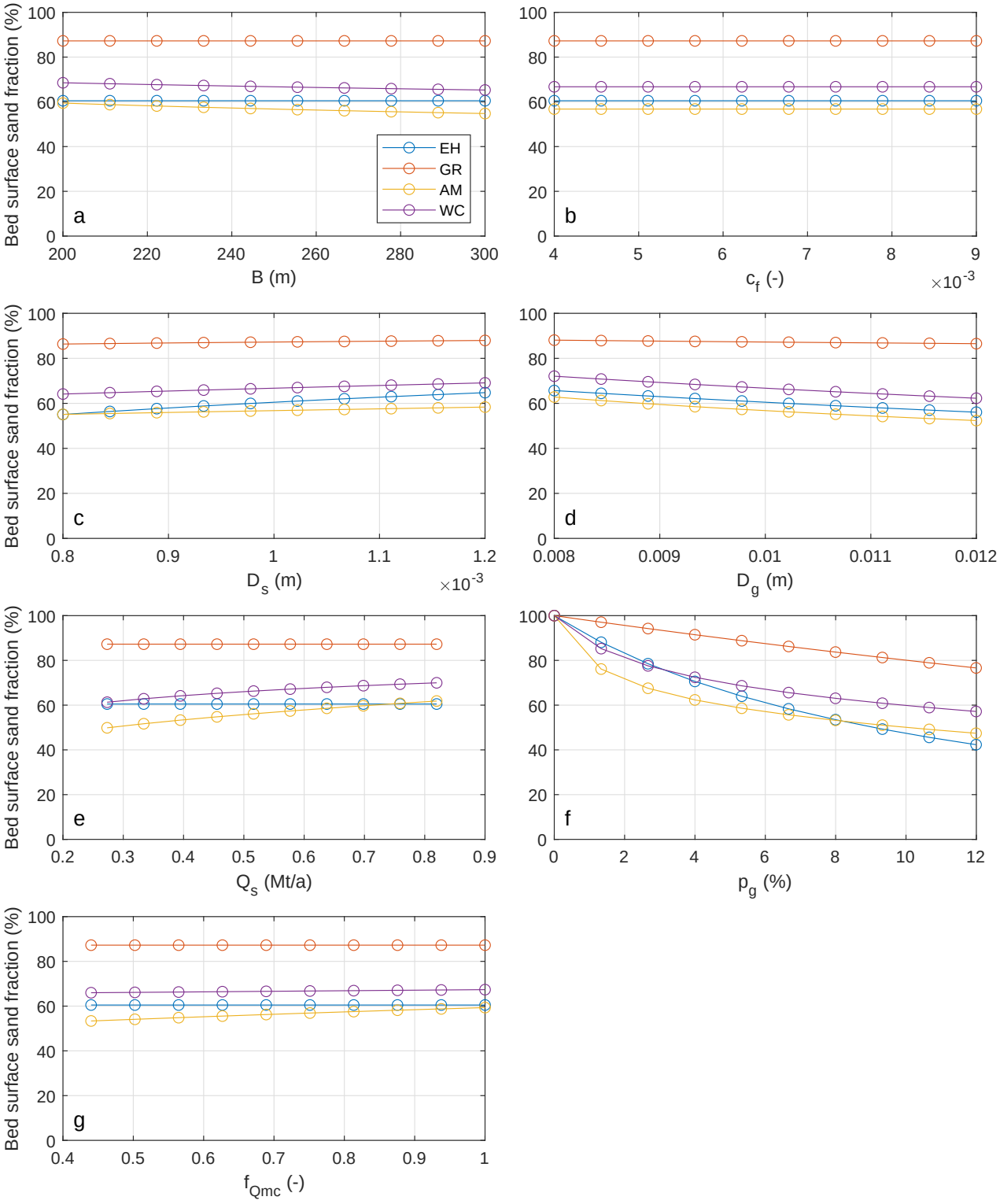

Figure 5.5: Sensitivity analysis of the equilibrium bed surface sand fraction for a varying: (a) channel width, (b) friction coefficient, (c) sand diameter, (d) gravel diameter, (e) total sediment supply, (f) mean gravel content in total sediment supply and (g) main channel discharge fraction. The calculations are based on the Engelund and Hansen (1967) load relation (EH), the generalized load relation (GR, where r = 0.05, $w_g = w_s = w$ = 0.4 and c = 2.3), the Ashida and Michiue (1972) load relation (AM) and the Wilcock and Crowe (2003) load relation (WC).

The influence of a larger parameter on the equilibrium bed slope results in either a constant or an increasing equilibrium bed surface sand fraction for the sand diameter, total sediment supply and main channel discharge fraction. The equilibrium bed surface sand fraction remains constant or decreases for a larger main channel width, gravel diameter and mean gravel content of the total sediment supply. The bed surface sand fraction remains constant for every friction coefficient value. In all cases, except for the mean gravel content, the GR load relation results in the highest bed surface sand fractions, followed by the WC load relation and subsequently by the EH load relation. The AM load relation results in the smallest bed surface sand fractions.

When considering the sensitivity of both the equilibrium bed slope and the equilibrium bed surface sand fraction, it appears that the mean gravel content of the total sediment supply has the most influence on the equilibrium state calculations, as it has the most influence on the equilibrium bed surface sand fraction and partially the most influence on the equilibrium bed slope. The input parameter that also has relatively much influence on both the equilibrium bed slope and the equilibrium bed surface sand fraction is the total sediment supply. The other parameters have less influence on the sensitivity of the calculated equilibrium state.

5.3. Results uncertainty analysis

This section presents the results from the Monte Carlo simulations for the uncertainty analysis as described in Section 4.5.

With the Monte Carlo analysis the equilibrium bed slope and the equilibrium bed surface sand fractions are calculated 100,000 times for each sediment transport relation, where every simulation is based on a different combination of input parameters values. Due to this high number of simulations, the calculated equilibrium bed slopes and equilibrium bed surface sand fractions represent a bandwidth of possible equilibrium state solutions. For each of these bandwidths, the 5% and 95% quantiles are calculated, which represent respectively the edge where there is a 5% confidence that the calculated solution is lower and a 5% confidence that the calculated solutions is higher than that value. The area between the 5% and 95% confidences is defined here as the 90% confidence interval, which means that there is a confidence of 90% that the calculated solution is within that area, and thus that the chance is high that the actual equilibrium state for the considered input parameters is within that area. These intervals are an indication of the uncertainty; the larger the interval size, the higher the uncertainty of the predicted equilibrium state is.

The calculated equilibrium bed slope solutions of the Monte Carlo analysis are represented by the boxplots in Figure 5.6. The upper whiskers indicate the 95% quantile and the lower whiskers the 5% quantile, the distance between these upper and lower limits is the 90% confidence interval. The median bed slopes of each transport relation are represented by the red lines in Figure 5.6. There are bed slope outliers for all transport relations, ranging from a minimum value of $1.5 \cdot 10^{-5}$ to a maximum value of $12 \cdot 10^{-5}$, but they are not included in the boxplots for clarity.

The values of the median bed slope values for each of the four sediment transport relations is given in Table 5.1, including the difference between the median and the lower limit, the difference between the median and the upper limit and the 90% confidence interval. These 90% confidence intervals are all approximately the same size, which means that the four sediment transport relations lead to similar uncertainties of the equilibrium bed slope predictions. When averaged over the four sediment transport relations, the equilibrium bed slope is approximately $1.8 \cdot 10^{-5}$ smaller or larger than the median values, with a 90% confidence interval of approximately $3.7 \cdot 10^{-5}$.

The result of the Monte Carlo analysis for the equilibrium bed surface sand fraction is given in Figure 5.7, which also has whiskers that represent the 95% and 5% quantiles. The outliers have been removed from this boxplot as well. For all four sediment transport relations calculations there is more sand than gravel in the bed surface composition when looking at the median bed surface sand fractions, which corresponds to the deterministic equilibrium bed surface sand fraction calculations (Figure 5.3). The 5% quantiles of the EH and AM load relations however indicate that there are also solutions possible where the bed surface sediment composition consists out of more gravel than sand.

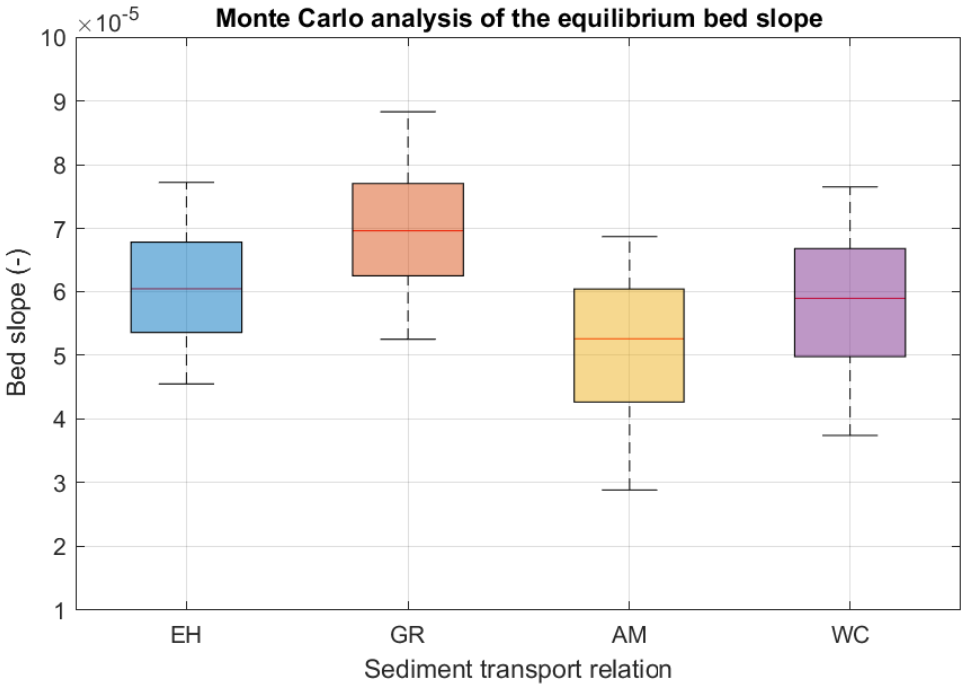

Figure 5.6: Boxplot of the Monte Carlo analysis results for the equilibrium bed slope. The upper whiskers indicate the 95% quantile and the lower whiskers indicate the 5% quantile. The outliers have been removed for clarity. The calculations are based on the following sediment transport relations: Engelund and Hansen (1967) (EH), a generalized load relation (GR, where r = 0.05, $w_g = w_s = w$ = 0.4 and c = 2.3), Ashida and Michiue (1972) (AM) and Wilcock and Crowe (2003) (WC).

Table 5.1: The median values of the bed slope for each sediment transport relation, the distance from the median to the lower limit and to the upper limit, and the 90% confidence interval.

	Median	Median to lower limit	Median to upper limit	90% confidence interval
EH	$6.0 \cdot 10^{-5}$	$-1.5 \cdot 10^{-5}$	$+1.7 \cdot 10^{-5}$	$3.2 \cdot 10^{-5}$
GR	$7.0 \cdot 10^{-5}$	$-1.7 \cdot 10^{-5}$	$+1.9 \cdot 10^{-5}$	$3.6 \cdot 10^{-5}$
AM	$5.3 \cdot 10^{-5}$	$-2.4 \cdot 10^{-5}$	$+1.6 \cdot 10^{-5}$	$4.0 \cdot 10^{-5}$
WC	$5.9 \cdot 10^{-5}$	$-2.1 \cdot 10^{-5}$	$+1.8 \cdot 10^{-5}$	$3.9 \cdot 10^{-5}$

The values of the median bed surface sand fractions for the different sediment transport relations is given in Table 5.2, which also includes the difference between the median and the lower limit, the difference between the median and the upper limit and the 90% confidence interval. There is quite some difference between the 90% confidence intervals of the different transport relations. The GR load relation has a relatively low range of uncertainty for the bed surface sand fractions, while the EH load relation leads to the largest range of uncertainty in the predicted bed surface sand fractions.

Table 5.2: The median values of the bed surface sediment composition for each sediment transport relation, the distance from the median to the lower limit and to the upper limit, and the 90% confidence interval.

	Median	Median to lower limit	Median to upper limit	90% confidence interval
EH	61%	-17%	+33%	51%
GR	88%	-10%	+11%	21%
AM	56%	-9%	+27%	37%
WC	67%	-9%	+25%	34%

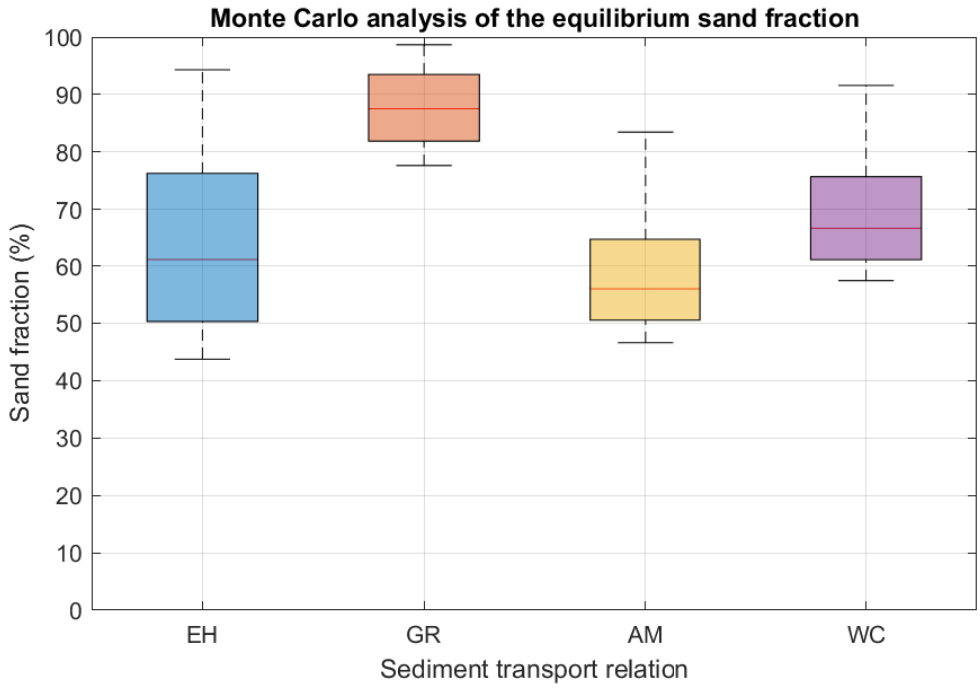

Figure 5.7: Boxplot of the Monte Carlo analysis results for the equilibrium bed surface sand fraction. The upper whiskers indicate the 95% quantile and the lower whiskers indicate the 5% quantile. The outliers have been removed for clarity. The calculations are based on the following sediment transport relations: Engelund and Hansen (1967) (EH), a generalized load relation (GR, where r = 0.05, $w_g = w_s = w$ = 0.4 and c = 2.3), Ashida and Michiue (1972) (AM) and Wilcock and Crowe (2003) (WC).

5.4. Comparison of equilibrium prediction and measured state

In this section, the measured state of the river Waal is compared to the calculations of the predicted equilibrium state. The measured bed slopes are introduced in Section 3.4, and the measured bed surface sediment composition is identified in Section 3.5. For the equilibrium state predictions, the results from the deterministic analysis in Section 5.1 are combined with the results from the uncertainty analysis in Section 5.3 to include both the spatial variations and the uncertainty related to the calculated equilibrium state.

On the left side of Figure 5.8, the measured bed slope of the river Waal from Figure 3.12 and the calculated deterministic equilibrium bed slopes from Figure 5.1 are plotted. The right side of Figure 5.8 shows the 90% confidence intervals from Figure 5.6, where each boxplot corresponds to the deterministic equilibrium bed slope that is calculated with the same sediment transport relation. The confidence intervals are a rough indication of how much steeper or milder the deterministic equilibrium bed slopes can be for the equilibrium state of the river Waal. If the deterministic bed slope at a certain location is larger than the median value of the corresponding boxplot, then the 90% confidence interval whiskers are estimated to be also that much higher. If the deterministic bed slope is lower at a certain location than the median value, then the 90% confidence interval whiskers are also expected to be lower. This is a rough estimation that is only used for a global idea of the uncertainty ranges corresponding to the deterministic equilibrium bed slopes.

It is clearly visible on the left side of Figure 5.8 that the measured bed slope is everywhere larger than the deterministic equilibrium bed slopes. It also appears that even when the deterministic bed slopes are combined with the uncertainty ranges at the right side of the figure, that the measured bed slope is steeper than the predicted equilibrium bed slopes for all four sediment transport relations.

The measured bed slope has larger variations along the river Waal than the deterministic equilibrium bed slopes. The measured bed slope is steepest at the border with the backwater segment at rkm 920, becomes milder towards rkm 915, and is approximately constant between rkm 915 and 885 except for a somewhat milder slope around rkm 902. The pattern of the equilibrium bed slopes is discussed in Section 5.1. There is

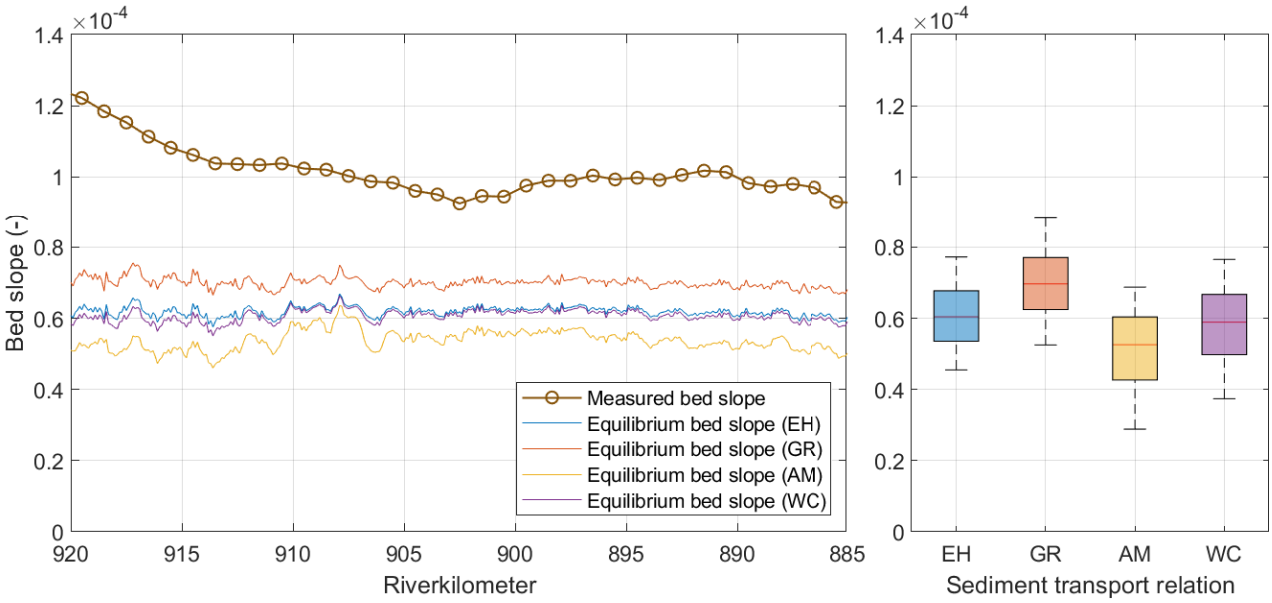

Figure 5.8: Comparison of the calculated deterministic equilibrium bed slopes and measured bed slope on the left side. The right side shows the 90% confidence intervals that correspond to the deterministic equilibrium bed slopes.

no obvious explanation for the different spatial patterns of the measured and the equilibrium bed slopes. A possibility could be that the model lacks spatial variations of certain input parameters, such as for instance the friction coefficient, that influence variations in the measurements of the bed slope along the river Waal. Another possibility could be that the model cannot represent the bed slope very well near the backwater segment. A third possibility is that there are less spatial differences in the bed slope when the river Waal has reached its equilibrium state.

The left side of Figure 5.9 shows the measured bed surface sand fraction of the river Waal from Figure 3.14 and the calculated deterministic equilibrium bed surface sand fractions form Figure 5.3. On the right side of Figure 5.9 the 90% confidence intervals for the equilibrium bed surface sand fractions from Figure 5.7 are given. For each sediment transport relation there is one deterministic equilibrium bed surface fraction that matches with one boxplot, indicated by the same colours. In this case, the confidence intervals are a rough indication of how different the ratio of the sand and gravel can be in the bed surface sediment composition for the equilibrium state of the river Waal. The same principle for the application of the 90% confidence intervals at the bed slopes is used here; it is assumed that for a bed surface sand fraction that is larger or smaller than the median value of the boxplot, the whiskers of the 90% confidence interval move accordingly.

The difference between the spatial variations of the measured and the calculated equilibrium bed surface sand fractions is striking. The measured bed surface sand fraction is relatively small at rkm 885 and becomes increasingly larger towards rkm 920, whereas the equilibrium bed surface sand fractions remain relatively constant. The spatial variation in the measurements can be explained by the migrating gravel-sand transition, as analysed in Section 3.2. That this spatial variation is not present in the calculated equilibrium bed surface sand fractions is probably due to the average sediment supply that is used in the model. If the sediment supply would vary along the river Waal in the model, then the calculated equilibrium sand fraction would have a similar spatial variation as the measured bed surface sand fraction. This is however not applied because it is conflicting with the equilibrium state definition that all sediment that enters the river upstream is transported downstream, as is explained in Section 4.3.

From the comparison of the measured and predicted equilibrium bed surface sand fractions without uncertainties on the left side of Figure 5.9, it can be deduced that the sand fraction calculated with the generalized load relations is everywhere higher than the measured sand fraction. However, whether the sand fractions from the other sediment transport relations are higher than the measured sand fractions depends on the location. At the most upstream part of the normal flow segment of the river Waal, between rkm 885 and 895, the

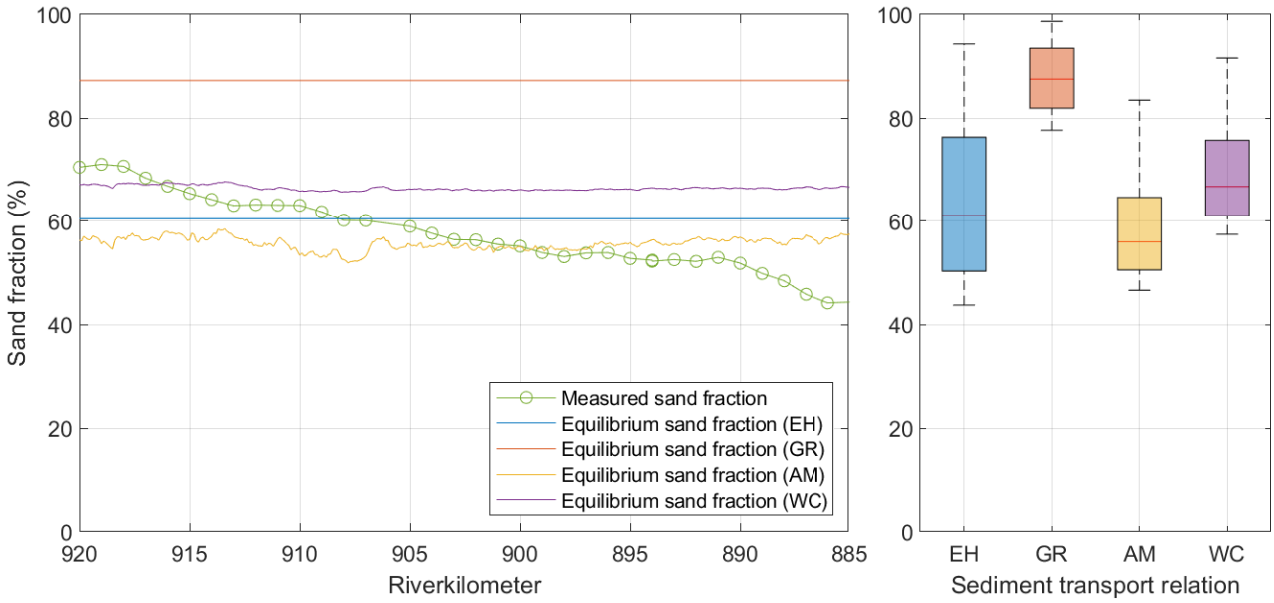

Figure 5.9: Comparison of the calculated deterministic equilibrium bed surface sand fractions and measured bed surface sand fraction on the left side. The right side shows the 90% confidence intervals that correspond to the deterministic equilibrium bed surface sand fractions.

measured sand fraction is lower than all deterministic sand fractions. From rkm 895 towards the downstream direction, the measured sand fraction becomes gradually larger than the equilibrium sand fractions for the EH, AM and WC load relations.

When the 90% confidence intervals of the bed surface sand fractions are considered, the measured bed surface sand fraction is at almost all locations within the uncertainty range of the EH and AM load relations. The measured bed surface sand fraction is lower than the equilibrium bed surface fractions corresponding to the WC load relation at the upstream half of the normal flow segment, roughly between rkm 885 and rkm 900. At the downstream end, the measured bed surface sand fractions also lie within the uncertainty range of the WC load relation. The measured bed surface sand fraction is everywhere smaller than the uncertainty range of the equilibrium bed surface sand fractions calculated with the GR load relation.

6

Discussion

This chapter discusses the impact of several assumed input parameter values and chosen approaches in Section 6.1, and reflects on the results of the equilibrium state calculations in Section 6.2.

6.1. Impact of assumptions and choices

This section discusses the impact that certain assumptions have on the calculated equilibrium river states. First the impact of the chosen friction coefficient is examined. Subsequently the effect that the input parameter values have on the applicability of the sensitivity and uncertainty analyses for other rivers is discussed. And finally, the impact of the approach for the Monte Carlo analysis is discussed.

6.1.1. Friction coefficient

The deterministic value for the friction coefficient that is used in this research is a spatially constant value of 0.0061, which is an assumption based on the thesis by Van Vuren (2005). A matching uncertainty range was chosen by using the uncertainties she describes in her thesis. However, the friction coefficient could also have another value, or it could even vary along the river Waal due to for instance a dependence on other parameters such as the water discharge. The chosen uncertainty range does not capture all these possible values for the friction coefficient. We look at the average friction coefficients used in the research by Arkesteijn et al. (2019) and Warmink (2011) to assess what the impact would be on the calculated equilibrium states if other values for the friction coefficient were used.

If the friction coefficient would have been based on Arkesteijn et al. (2019), the average value would have been 0.007 instead of 0.0061, which falls inside the used uncertainty range. From the results of the sensitivity analysis it can be concluded that the equilibrium bed slope would have been approximately $0.5 \cdot 10^{-5}$ smaller for the GR, AM and WC load relations, and approximately equal for the EH load relation. Similar results would have also been expected for the Monte Carlo analysis. This difference is considered to be small. There are no consequences for the bed surface sediment composition, because it is not related to the friction coefficient (Figure 5.5). Using the friction coefficient by Arkesteijn et al. (2019) would therefore lead to similar equilibrium state predictions with respect to the equilibrium state predictions in Chapter 5, and also to similar findings for the comparison of the calculated equilibrium states with the river state measurements.

The difference would have been larger if the friction coefficient would have been based on Warmink (2011). The exact friction coefficient is more difficult to determine, because the friction is given by the Nikuradse roughness and depends on the magnitude of the water discharge. To transform the Nikuradse roughness into a friction coefficient, the hydraulic radius must be known, which also depends on the water discharge. For the mean discharge at Lobith of 2200 m^3/s, with a hydraulic radius of approximately 6 m as was calculated

in Section 4.1, the Nikuradse roughness is approximately 0.05 according to Figure 4.2 from Warmink (2011). This results in a friction coefficient of 0.003, which is even lower than the lowest value from the uncertainty distribution in Figure 4.7. The predicted channel slope would then be drastically higher, going towards $10 \cdot 10^{-5}$ (Figure 5.4). This would have consequences for the answer to the main research question, because the equilibrium bed slope would then be very close to the measured bed slope, except for the Engelund and Hansen (1967) load relation, which would make it less clear whether the calculated equilibrium bed slope matches the expectation from Section 3.2. It is still assumed that the friction coefficient by Van Vuren (2005) that is used in this study is a good assumption, however with this knowledge of the impact that a friction coefficient based on the research from Warmink (2011) can have on the research questions, it is recommended to further investigate the influence of the friction coefficient.

6.1.2. Applicability results on other rivers

The equilibrium state calculations in this report are based on input parameter values that are representative for the river Waal. As a consequence, the sensitivity analysis is not directly applicable to other rivers. However, the results of the sensitivity analysis give insight in the order of magnitude for the uncertainty in the equilibrium state for a certain parameter uncertainty range. This can help make a first estimation of the parameter uncertainties that contribute most to the uncertainty of the predicted equilibrium state.

The results of the uncertainty analysis are also only directly applicable to the river Waal. These results could be used as a first estimate of the range of uncertainties that can be expected when using the analytical relations. However, we do not recommend to apply this range to any other river than the river Waal, mainly for two reasons:

- We expect that the three uncertainty distributions that have been used in the uncertainty analysis are not the same for other rivers, due to for instance different mean values and other measurement uncertainties. Moreover, it is possible that the three input parameters in the uncertainty analysis for the river Waal are not the most important parameters for another river, which would mean that relevant uncertainty sources are not included in the uncertainty analysis.
- The equilibrium state values do not depend linearly on all input parameters, which means that the influence of a different input parameter value on the equilibrium state can not easily be deduced, especially in the Monte Carlo analysis where 100,000 different input value combinations are calculated.

6.1.3. Monte Carlo analysis

A limitation of the Monte Carlo analysis is that the distributions that are used are rough assumptions, and might therefore either overlook possible equilibrium state predictions or include unnecessary uncertainties. For example, the chance that the mean gravel content is zero is as high as any other value due the uniform distribution, even though it is very unlikely given the amount of gravel that is measured at the bed surface. Next to that, there are no correlations included that are perhaps present, for example between the total sediment supply and the mean gravel content of the total sediment supply.

Furthermore, the Monte Carlo analysis includes only three uncertainty distributions. The chosen three input parameters lead to the largest uncertainties in the sensitivity analysis, implying that these parameters have indeed the most influence on the uncertainty of the equilibrium state. However, more input parameter uncertainties could have been included, which would have resulted in a better representation of the possible equilibrium states.

Due to these limitations, the outcome of the Monte Carlo analysis should not be seen as a perfect representation of all possible equilibrium states, but as an indication of the range of uncertainties. Because the aim of this study is to get an impression of where the equilibrium state is with respect to a base case, this approach suffices and these limitations do not have consequences for the outcome of this study.

6.2. Reflection on results

This section reflects on the results of the equilibrium state calculations. First, the mismatch between the expectations and the results of the measured and equilibrium state comparison is discussed. This is followed by a discussion on what the results can be used for. Finally, the absence of uncertainties in the measured state of the river Waal is discussed.

6.2.1. Mismatch expectations and results comparison

The expectations for the equilibrium state of the river Waal, as analysed in Section 3.2, are that the equilibrium bed slope is milder than the current bed slope, and that the equilibrium bed surface sand fraction is smaller than the current bed surface sand fraction.

The results of the comparison between the calculated equilibrium state and the measured state of the river Waal in Section 5.4 show that the equilibrium bed slope is milder than the measured bed slope, and that the equilibrium bed surface sand fraction is either larger than or too uncertain to compare it with the measured bed surface sand fraction.

When these expectations and results are compared, it appears that the expectation of the equilibrium bed slope corresponds to the results, however the expectation of the equilibrium bed surface sand fraction does not match with the results. We give four possible explanations for this mismatch, based on the results of the sensitivity analysis in Section 5.2:

1. The mean gravel content of the total sediment supply could be underestimated. It could be possible that the approach of averaging the sediment input and sediment output of the river Waal has led to an underestimation of the gravel content of the total sediment supply, because no gravel leaves the river Waal according to Frings et al. (2015). It could be reasoned that the total sediment supply that currently enters the river Waal, will in future equilibrium state conditions also exit the river Waal, leading to a mean gravel content of approximately 11% in the total sediment supply. This would lead to a decrease in the deterministic bed surface sand fraction of 5% to 15% according to Figure 5.5, which would make most of the deterministic equilibrium bed surface sand fractions smaller than the measured bed surface sand fraction. This is a better match with the expectations, however the impact on the uncertainty range of the bed surface sand fraction and the increase of the bed slope due to a higher gravel content of the total sediment supply should be considered.
2. The total sediment supply could have been overestimated. However, this would lead to at most a reduction of 0% to 10% of the deterministic equilibrium bed surface sand fraction (Figure 5.5), which is not enough to fully explain the mismatch.
3. The gravel diameter could have been larger. When looking at the sensitivity analysis, the bed surface sand fraction could be at most 10% lower due to a larger gravel diameter, which is similarly to the previous explanation not enough to justify the mismatch.
4. The sand diameter could have been smaller. A smaller sand diameter results in a lower bed surface fraction (Figure 5.5), however the reduction is at most 5%. This is again not enough to explain the mismatch.

Next to these four explanations based on the sensitivity analysis, it is also possible that the values of the input parameters are not representative for the river Waal, or that the assessment that the equilibrium bed surface sand fraction is smaller in the equilibrium state is wrong. We consider the first explanation to be the most likely reason for the mismatch.

6.2.2. Use of the results

The result of the sensitivity analysis shows which input parameter variations lead to the largest uncertainties in the predicted equilibrium states of the river Waal. This information can be used to decide for which parameters a reduction in uncertainty would be worthwhile, and thus for which input parameters more research is

beneficial. The extent of such research depends on the desired level of uncertainty reduction of the predicted equilibrium state.

The result of the uncertainty analysis shows the 90% confidence interval of possible equilibrium states for variable input parameter scenarios. This bandwidth indicates which values for the equilibrium bed slope and equilibrium bed surface sand fraction can represent the equilibrium state that corresponds to the given input parameters. This does not mean that the equilibrium state of the river Waal is almost certainly within this bandwidth, because the input parameters could be not representative for the river Waal, and because we have not investigated how well the analytical relations are able to predict an equilibrium state. The uncertainty bandwidth can however be used as an indication of the influence that the uncertainty of the input parameters has on the equilibrium state calculations. This is useful knowledge for the assessment whether an equilibrium state prevails along the river Waal.

6.2.3. Uncertainty in measured state of river Waal

In this research, the uncertainty that is related to the measured bed slope and bed surface sediment composition is absent in the comparison with the calculated equilibrium state. It is therefore for example possible that the calculated equilibrium bed slope is not at every location milder than the measured bed slope, and that the calculated equilibrium bed surface sand fraction is at some locations smaller than the measured bed surface sand fraction. This would however not lead to different conclusions for the main research question, as the expectations for the calculated equilibrium state are already not met. Furthermore, this study does not investigate how the river Waal will change based on equilibrium state calculations.

If the analytical relations are used in a future research to predict the equilibrium state of a river, the uncertainties in the measured state are important to include, to ensure that all possible scenarios for the future river state are considered.

7

Conclusion and recommendations

This chapter explains the conclusion and recommendations of this study. Section 7.1 describes the conclusion by first answering the sub-questions and then the main research question. Section 7.2 gives recommendations for further studies.

7.1. Conclusion

This section first answers the four sub-questions, and subsequently gives the conclusion of the main research question.

7.1.1. Sub-questions

1. *What is the range of applicability of the analytical relations?*
The analytical relations by Blom et al. (2017) are used in this research to predict the equilibrium state of the river Waal. These relations are based on certain assumptions and they have a limitation under which circumstances they can be applied. We have analysed what the influence of these assumptions and limitation is on the river Waal, to assess how well these relations can be applied to the case study.

The conclusion of this analysis is that the analytical relations are in general well applicable to the river Waal. Most of the assumptions are found to be acceptable, because it is assumed that their influence on the equilibrium state predictions is small enough to have no significant impact on the research questions. There are however three points of attention;

1. Normal flow segment limitation
   The analytical relations are only applicable on normal flow segments, thus outside the HBL and backwater segments. The normal flow segment of the river Waal is identified in this research to be able to apply the analytical relations. This region is approximately 35 km, whereas the total length of the river Waal is about 90 km, which means that less than 50% of the river Waal could be included as study area.
2. No floodplains
   The analytical relations assume that there are no floodplains, meaning that all water remains in the main channel. Because the floodplains play an important role for the river Waal, their interaction with the main channel is mimicked by multiplying the water discharge with a factor that represents the water that remains in the main channel as a function of the discharge magnitude and location along the river Waal. Due to this factor the effect of the floodplains was included in the equilibrium state calculations.
3. Independence of the friction coefficient
   The last point of attention is the assumption that the friction coefficient is independent of the bed surface

sediment composition and local flow parameters. This assumption is likely not true, but it is not known what the impact of this assumption is on the equilibrium state calculations, nor is there a straightforward method to include these dependencies. The assumption is therefore adopted, but it is recommended to investigate the effect of friction coefficient dependencies on equilibrium state calculations.

2. *How sensitive is the predicted equilibrium state to uncertainty in the input parameters?*
A model is set-up in this study that predicts the equilibrium state of a river based on the analytical relations. The equilibrium state of an engineered river is characterized by its equilibrium bed slope and equilibrium bed surface sediment composition. A sensitivity analysis is performed to identify which input parameters of the model result in the largest variation of possible equilibrium states for the river Waal.

The result of the sensitivity analysis for the bed slope is that the equilibrium bed slope is sensitive to all seven considered input parameters; the main channel width, the friction coefficient, the sand diameter, the gravel diameter, the total sediment transport, the mean gravel content in the total sediment transport and the main channel discharge fraction. However, the equilibrium bed slope of the river Waal is most sensitive to the uncertainty of the total sediment transport and the mean gravel fraction in the total sediment transport. To which of these input parameters the bed slope is most sensitive depends on the sediment transport relation.

The equilibrium bed surface sand fraction of the river Waal is by far the most sensitive to the mean gravel fraction of the total sediment transport. The uncertainty ranges of the sand diameter, gravel diameter and total sediment transport can also lead to some uncertainty in the equilibrium bed surface sand fraction predictions, depending on the sediment transport relation. The other considered input parameters have no or negligible impact on the equilibrium bed surface sand fraction predictions of the river Waal.

The conclusion is that the mean gravel fraction of the total sediment transport results in the highest uncertainty of the equilibrium state of the river Waal, followed by the total sediment transport. Reducing the uncertainty of the mean gravel fraction of the total sediment transport would be an effective way to decrease the uncertainty of the equilibrium state of the river Waal.

3. *What is the range of uncertainty of the predicted equilibrium state?*
A Monte Carlo analysis is performed to identify the possible equilibrium states of the river Waal. For this analysis, a normal distribution for the total sediment transport, a lognormal distribution for the friction coefficient and a uniform distribution for the mean gravel content in the total sediment transport are used. The other input parameters are kept constant at their average values. From the Monte Carlo analysis a 90% confidence interval is defined for both the equilibrium bed slope and the equilibrium bed surface sand fraction, which represents the uncertainty range of the predicted equilibrium state.

The conclusion from this analysis is that the equilibrium bed slope can be approximately $1.8 \cdot 10^{-5}$ smaller or larger than the deterministic bed slope, with a 90% confidence interval of approximately $3.7 \cdot 10^{-5}$. The equilibrium bed surface sand fraction can be approximately 10% to 20% smaller and 10% to 35% larger than the deterministic bed surface sand fraction, with a 90% confidence interval between 20% to 50%, depending on which sediment transport relation has been used.

4. *How does the predicted equilibrium state compare to measured data?*
The predicted deterministic equilibrium bed slope of the river Waal is for all sediment transport relations smaller than the measured bed slope. Even when the uncertainty ranges of the equilibrium bed slopes are considered, the predicted bed slopes are milder than the measured bed slope.

Whether the predicted deterministic equilibrium bed surface sand fractions are larger or smaller than the measured bed surface sand fraction depends on the sediment transport relation and the location along the river Waal. The measured bed surface sand fraction is smaller than the equilibrium predictions at the upstream end of the considered case study area, whereas the measured bed surface sand fraction is larger than most equilibrium predictions at the downstream end of the case study. When the uncertainty ranges of the equi-

librium bed surface sand fractions are considered, the measured bed surface sand fraction falls within these uncertainty ranges along at least half of the study area for three sediment transport relations. This means that in this region the measured bed surface sand fraction can be equal to or smaller/larger than the equilibrium bed surface sand fraction predictions. Only for one sediment transport relation is the predicted equilibrium sand fraction including uncertainties everywhere higher than the measured bed surface sand fraction.

7.1.2. Main research question

The main research question is: *How well can we assess whether an equilibrium state prevails along a river reach?*

We answer the main research question by first assessing the range of uncertainty, subsequently by analysing whether the results of the comparison of the calculated equilibrium state and measured state are as expected, and finally by combining these findings into a conclusion.

We estimate that the range of uncertainty of the equilibrium bed slope calculations is acceptable for a rough prediction of the equilibrium state of the river Waal, because we assume that a more precise answer would probably not lead to large differences in the assessment of the presence of an equilibrium state. On the other hand, we estimate that the range of uncertainty of the equilibrium bed surface sand fractions is quite large, because it ranges from a possibility that more gravel than sand is present at the river bed, to a possibility that the bed surface consists of almost no gravel. We consider this range of uncertainty too large to assess whether an equilibrium state prevails along the river Waal.

It is deduced from measurements of the bed slope, the bed surface grain size and the sediment transport that the river Waal has not yet reached its equilibrium state. This implies that the comparison between the predicted equilibrium and measured state of the river Waal should show that the bed slopes and bed surface sand fractions are not equal. Furthermore, the measured bed slope decrease suggests that the river Waal is currently heading towards a milder bed slope, which implies that the equilibrium bed slope is expected to be lower than the measured bed slope. Similarly, it is expected that the equilibrium bed surface sand fraction is lower than the measured bed surface sand fraction, due to the measured coarsening of the median grain size.

Regarding the bed slopes, it is indeed found that the equilibrium bed slope, including uncertainties, is smaller than the measured bed slope along the entire case study area. Considering the bed surface sand fractions, it is either not known what the difference is between the measurements and equilibrium predictions due to the uncertainty ranges, or the equilibrium bed surface sand fractions appear to be higher than the measurements. This does not correspond to the expectation that the equilibrium bed surface sand fractions are lower.

It appears from the above findings that 1) the uncertainty range of the calculated bed surface sand fractions is considered to be too large to predict the equilibrium state of the river Waal, and 2) the equilibrium bed surface sand fraction predictions do not match the expectation. The conclusion is therefore that the current model equilibrium state predictions are not yet good enough to assess whether an equilibrium state prevails along the river Waal.

7.2. Recommendations

This section gives recommendations on three topics; improvements on the equilibrium state calculations, further research with another set of analytical relations, and the approach for further research on equilibrium state predictions.

7.2.1. Improvements on equilibrium state calculations

We have four recommendations to improve the equilibrium state identification of the river Waal:

- Assess why there is a mismatch between the expected and calculated bed surface sand fractions. Section 6.2 in the Discussion gives an overview of possible explanations of the mismatch, of which we consider a different mean gravel content of the total sediment supply to be the most likely reason. Research on what the cause is of the mismatch can be used to improve the equilibrium bed surface sand fraction calculations, and therefore also the equilibrium state identification of the river Waal.
- Perform research to reduce the input uncertainty. The uncertainty range of the equilibrium bed surface sand fractions is considered to be too large to identify an equilibrium state. To reduce this range, it is recommended to reduce the uncertainty of the mean gravel content of the total sediment supply, for example with more frequent measurement campaigns of the bed surface sediment composition of the river Waal. It is also recommended to investigate which of the sediment transport relations used in this study is more reliable for the equilibrium state calculations, to reduce the range of equilibrium bed surface sand fractions.
- Validate the equilibrium state predictions. It is recommended to check whether other predictions of the equilibrium state of the river Waal match with the predictions made with the analytical relations in this study. This can be done by comparing the computed equilibrium state to trustworthy numerical model simulations of an equilibrium state, or to calculations of other analytical relations, such as the relations by Arkesteijn et al. (2019).
- Perform more research on the friction coefficient. We have encountered three issues with the friction coefficient, and we recommended the following steps to improve them: 1) the analytical relations are based on the assumption that the friction coefficient is independent of the bed surface texture and local flow parameters. This is likely not true, however the impact that this assumption has on the equilibrium state predictions is not known. We recommended to research what the influence of these dependencies would be on the equilibrium state predictions, and whether ignoring the dependencies would lead to acceptable results. 2) it is found in the sensitivity analysis that the equilibrium bed slope decreases for an increasing friction coefficient for three of the sediment transport relations. This is an unexpected behaviour that cannot be explained. We recommended to examine whether this behaviour is due to an error in the model. 3) it is found in the Discussion that using another source for the friction coefficient can lead to such different calculations that it has impact on the answer of the main question. We recommended to investigate which range of friction coefficient values represent the river Waal the best.

7.2.2. Further research with other analytical relations

The analytical equilibrium relations by Blom et al. (2017) have been investigated in this research, however the analytical equilibrium relations by Arkesteijn et al. (2019) would have been a good alternative as explained in Section 2.2. We recommend to use these relations in new research for the following goals:

- To validate the results of the equilibrium state calculations in this study. This can be done by first calculating the equilibrium state of the river Waal with the relations by Arkesteijn et al. (2019) for the same input parameters, and by subsequently comparing it to the equilibrium state calculations in Chapter 5.
- To investigate what the equilibrium state is on the backwater segment of the river Waal, and how well it can be assessed whether an equilibrium state prevails there.
- To assess what the difference is between equilibrium state calculations at a backwater segment for the two different sets of analytical relations. This can help to evaluate how well the analytical relations by Blom et al. (2017) can be used on backwater segments; can they be used as a first estimate, or should predictions on backwater segments with these relations be prevented.

7.2.3. Approach for further research on equilibrium state predictions

There are two subjects that we recommended to pay attention to if a study is performed in the future where the equilibrium state of a river is predicted to investigate the effect of an intervention:

- Base case for interventions
  The calculated equilibrium state is in this research compared to measurements of the river Waal as a base case. This type of base case can be used to investigate whether the river has reached its equilibrium state, but also how the river will respond to a new intervention by comparing it with predictions of the equilibrium state including this intervention. However, another possibility to investigate the impact of an intervention would be to use equilibrium state calculations of the river before the intervention as a base case. The advantage of the current base case is that it gives a better impression of the changes that a river will undergo in time. The second base case however is useful to assess what the impact of that intervention is, which can help decide if the intervention should be implemented or not.

- Spatial scale
  We recommended to make an estimation about the spatial scale that is required for the equilibrium state prediction if the research aim is to assess the impact of an intervention. In this study, only a part of the river Waal was included, the normal flow segment. It could however be that an intervention has a negative impact on another part of the river Waal, for example further downstream in the backwater segment. Such an impact would not have been found due to the study area in this research, so we recommend to assess beforehand what the spatial scale is that is needed, and whether the analytical relations by Blom et al. (2017) can be applied on that case study or that another method is needed.

Bibliography

An, C., Fu, X., Wang, G., and Parker, G. (2017). Effect of grain sorting on gravel bed river evolution subject to cycled hydrographs: Bed load sheets and breakdown of the hydrograph boundary layer. *Journal of Geophysical Research: Earth Surface*, 122(8):1513–1533.

Arkesteijn, L., Blom, A., Czapiga, M. J., Chavarrías, V., and Labeur, R. J. (2019). The Quasi-Equilibrium Longitudinal Profile in Backwater Reaches of the Engineered Alluvial River: A Space-Marching Method. *Journal of Geophysical Research: Earth Surface*, 124(11):2542–2560.

Ashida, K. and Michiue, M. (1972). Study on hydraulic resistance and bed-load transport rate in alluvial streams. *Proceedings of the Japan Society of Civil Engineers*, 1972(206):59–69.

Battjes, J. A. and Labeur, R. J. (2017). *Unsteady Flow in Open Channels*. Cambridge University Press, Cambridge.

Blom, A., Arkesteijn, L., Chavarrías, V., and Viparelli, E. (2017). The equilibrium alluvial river under variable flow and its channel-forming discharge. *Journal of Geophysical Research: Earth Surface*, 122(10):1924–1948.

Blom, A., Viparelli, E., and Chavarrías, V. (2016). The graded alluvial river: Profile concavity and downstream fining. *Geophysical Research Letters*, 43(12):6285–6293.

Bolla Pittaluga, M., Luchi, R., and Seminara, G. (2014). On the equilibrium profile of river beds. *Journal of Geophysical Research: Earth Surface*, 119(2):317–332.

Buffington, J. M. (2012). Changes in channel morphology over human time scales [chapter 32]. In Church, M., Biron, P. M., and Roy, A. G., editors, *Gravel-Bed Rivers: Processes, Tools, Environments*, page 435–463. Wiley, Chichester, UK.

CBS (2018). Goederenvervoer in Nederland. `https://www.cbs.nl/nl-nl/maatschappij/verkeer-en-vervoer/transport-en-mobiliteit/transport/goederenvervoer/categorie-goederenvervoer/goederenvervoer-in-nederland`.

Church, M. and Ferguson, R. I. (2015). Morphodynamics: Rivers beyond steady state. *Water Resources Research*, 51(4):1883–1897.

De Vriend, H. (2015). The long-term response of rivers to engineering works and climate change. *Proceedings of the Institution of Civil Engineers: Civil Engineering*, 168(4):152–153.

De Vries, M. (1993). *Use of Models for River Problems*. UNESCO.

Doyle, M. W. and Shields, C. A. (2008). An alternative measure of discharge effectiveness. *Earth Surface Processes and Landforms*, 33(2):308–316.

Drinkwaterplatform (2020). Waar komt ons kraanwater vandaan? `https://www.drinkwaterplatform.nl/waar-komt-ons-kraanwater-vandaan/`.

Engelund, F. and Hansen, E. (1967). Monograph on sediment transport in alluvial streams. Technical report, Technical University of Denmark, Copenhagen, Denmark.

Fernández, R. and Garcia, M. H. (2017). Input-variable sensitivity assessment for sediment transport relations. *Water Resources Research*, 53(9):8105–8119.

Frings, R. M., Banhold, K., and Evers, I. (2015). Sedimentbilanz des Oberen Rheindeltas. Technical report, RWTH Aachen University, Aachen.

Frings, R. M., Hillebrand, G., Gehres, N., Banhold, K., Schriever, S., and Hoffmann, T. (2019). From source to mouth: Basin-scale morphodynamics of the Rhine River. *Earth-Science Reviews*, 196.

Howard, A. (1980). *Thresholds in river regimes.* cited By 155.

Howard, A. D. (1982). Equilibrium and time scales in geomorphology: application to sand-bed alluvial streams. *Earth Surface Processes and Landforms*, 7:303–325.

Jansen, P., Van Bendegom, L., Van den Berg, J., De Vries, M., and Zanen, A. (1994). *Principles of River Engineering*. Delftse Uitgevers Maatschappij.

Lanzoni, S., Luchi, R., and Bolla Pittaluga, M. (2015). Modeling the morphodynamic equilibrium of an intermediate reach of the po river (italy). *Advances in Water Resources*, 81:95–102. Fluvial Eco-Hydraulics And Morphodynamics.

Nones, M., Varrani, A., Franzoia, M., and Di Silvio, G. (2019). Assessing quasi-equilibrium fining and concavity of present rivers: A modelling approach. *Catena*, 181.

Paarlberg, A. J., Dohmen-Janssen, C. M., Hulscher, S. J., Termes, P., and Schielen, R. (2010). Modelling the effect of time-dependent river dune evolution on bed roughness and stage. *Earth Surface Processes and Landforms*, 35(15):1854–1866.

Reeze, B., van Winden, A., Postma, J., Pot, R., Hop, J., and Liefveld, W. (2015). Watersysteemrapportage Rijntakken 1990-2015. Technical report, Bart Reeze Water & Ecologie, Harderwijk.

Rudolph, M. (2018). *Measures for mitigating the ongoing bed degradation in the German and Dutch Rhine river - An indicative assessment using idealized models of the Waal branch*. PhD thesis, RWTH Aachen University.

Schielen, R. and Blom, A. (2018). A reduced complexity model of a gravel-sand river bifurcation: Equilibrium states and their stability. *Advances in Water Resources*, 121:9–21.

Ten Brinke, W. B. M. (1997). *De bodemsamenstelling van Waal en IJssel in de jaren 1996, 1976, 1984 en 1995*. Rijkswaterstaat.

Van Reen, M. (2002). *Morfologische problemen rond bochtverbeteringen in de Waal*. PhD thesis, Delft University of Technology.

Van Vuren, B. G. (2005). *Stochastic modelling of river morphodynamics*. PhD thesis, Delft University of Technology.

Vergouwe, R. (2015). The National Flood Risk Analysis for the Netherlands. Technical report, Rijkswaterstaat VNK Project Office.

Viparelli, E., Gaeuman, D., Wilcock, P., and Parker, G. (2011). A model to predict the evolution of a gravel bed river under an imposed cyclic hydrograph and its application to the Trinity River. *Water Resources Research*, 47(W02533).

Warmink, J. J. (2011). *Unraveling uncertainties*. PhD thesis, Delft University of Technology.

Wilcock, P. R. and Crowe, J. C. (2003). Surface-based Transport Model for Mixed-Size Sediment. *Journal of Hydraulic Engineering*, 129(2):120–128.

Ylla Arbós, C., Blom, A., Viparelli, E., Reneerkens, M., Frings, R. M., and Schielen, R. (2020). River Response to Anthropogenic Modification: Channel Steepening and Gravel Front Fading in an Incising River. *Geophysical Research Letters*, pages 1–10.

List of Figures

List of Tables

List of Abbreviations

Abbreviation	
AM	Ashida and Michiue (1972) load relation
EH	Engelund and Hansen (1967) load relation
GR	Generalised load relation
HBL	Hydrograph boundary layer
NAP	Normaal Amsterdams Peil
PDF	Probability density function
rkm	Riverkilometer
WC	Wilcock and Crowe (2003) load relation

List of Symbols

Symbol		
c_f	friction coefficient	-
C	Chézy coefficient	$m^{1/2}/s$
d	water depth	m
d_r	relative difference	%
D_{50}	median bed surface grain size	mm
D_{gravel}	gravel diameter	mm
D_{sand}	sand diameter	mm
g	gravitational acceleration	m/s^2
h	water surface	m
H	energy head	m
i_b	bed slope	-
i_f	friction slope	-
i_w	water surface slope	-
I_{up}	sediment input from upstream	Mt/a
O_{do}	sediment mass leaving the river	Mt/a
O_{dr}	sediment output due to dredging	Mt/a
O_{fl}	sediment output due to sedimentation on floodplains	Mt/a
Q	water discharge	m^3/s
Q_{s0}	sediment supply	Mt/a
$Q_{s0,gravel}$	gravel supply	Mt/a
$Q_{s0,sand}$	sand supply	Mt/a
$Q_{s0,total}$	total sediment supply	Mt/a
s	streamwise direction	-
u	flow velocity	m/s
z	elevation	m
z_b	bed elevation	m
ΔS	sediment mass stored in the river	Mt/a